International Journal on Interactive Design and Manufacturing (IJIDeM) (2020) 14:225–253
https://doi.org/10.1007/s12008-020-00650-3

ORIGINAL PAPER

A predictive tool to evaluate braking system performance using a fully coupled thermo-mechanical finite element model

Ali Belhocine[1] · **Asif Afzal**[2]

Received: 20 April 2019 / Accepted: 7 January 2020 / Published online: 18 January 2020

Abstract
The braking phenomenon is an aspect of vehicle stopping performance where with kinetic energy due to speed of the vehicle is transformed to thermal energy via the friction between the brake disc and its pads. The heat must then be dissipated into the surrounding structure and into airflow around the brake system. The frictional thermal field during the braking phase between the disc and the brake pads can lead to excessive temperatures. In our work, we presented a numerical modeling using ANSYS software adapted in the finite element method, to follow the evolution of the global temperatures for the two types of brake discs, full and ventilated disc during braking scenario. Also, numerical simulation of the transient thermal and the static structural analysis were performed here sequentially, with coupled thermo-structural method. Numerical procedure of calculation relies on important steps such that the Computational Fluid Dynamics (CFD) and thermal analysis have been well illustrated in 3D, showing the effects of heat distribution over the brake disc. This CFD approach helped in the calculation of the values of the thermal coefficients (h) that have been exploited in the 3D transient evolution of the brake disc temperatures. Three different brake disc materials were tested and comparative analysis of the results was conducted in order, to derive the one with the best thermal behavior. Finally, the resolution of the coupled thermomechanical model allows us to visualize other important results of this research such as; the deformations, and the equivalent stresses of Von Mises of the disc, as well as the contact pressure of the brake pads. Following our analysis and results we draw from it, we derive several conclusions. The choice allowed us to deliver the rotor design excellence to ensure and guarantee the good braking performance of the vehicles.

Keywords Brake disc · Pad · Finite element analysis · Thermomechanical coupling · Gray cast iron · Von Mises stress · Contact pressure

1 Introduction

Automobile is complex integration of electronic and mechanical components. One of the major components is the braking system which is limited due to its shortcomings. The translational movement of the brake pedal needs to be converted into the rotational movement of the airfoil blade to increase drag during the braking process. The precise calculation of the total heat generated by the friction between the automobile brake disc and the brake pads, as well as the distribution of this heat energy, is an essential step in the thermal analysis of the automotive braking system. The amount and distribution of the heat generated are depending on many variables such as the contact pressure, the coefficient of friction, sliding speed, etc. [1]. In addition, all the heat flux absorbed by the two bodies (disc and brake pads) is equivalent to the heat generated at their interface during emergency stop braking. Slice of frictional heat during the braking phase of vehicle is propagated in the atmosphere following two phenomena; in this case, radiation and thermal convection. As engineering systems become increasingly sophisticated, the complexity of the problems faced by engineers also increases. The lack of efficient physical models is one consequence of this complexity [2]. Heat transfer coefficients determine the intensity of the functional physical phenomena [3]. A model is an abstraction of reality and no

✉ Ali Belhocine
belhocine.2018@gmail.com

[1] Department of Mechanical Engineering, University of Sciences and the Technology of Oran (USTO), L.P 1505 El -MNAOUER, 31000 Oran, Algeria

[2] Department of Mechanical Engineering, P. A. College of Engineering, Mangaluru, India

model represents it perfectly. In mechanical engineering, as in other areas, it is possible to find a number of models to simulate the same phenomenon [4]. Models are the keystone of mechanical simulations. Generally, some aspects of reality are preferred over others, as in computer scene graphics simulation or finite element analysis simulations. But, in the case of interactive mechanical simulations, much more aspects have to be incorporated. Also, virtual reality deals with very large topics which have started from the CAD/CAE software, the development of innovative techniques for the modeling of product and systems behavior. It is obvious, therefore, that the calculation of the heat transfer coefficient (h) in simulation and numerical modeling is very serious. However, the latter is very much to evaluate; because of the complexity of friction phenomenon in the braking phase of automobiles. Automotive companies continuously strive to design better products faster and more cheaply using simulation models to evaluate every possible aspect of the product [5]. In a design context, lot of works focus on the research in interactive design [6]. Thanks to the advancement of computer technology, various models have been suggested in the past on interactive design and manufacturing [7]. As an alternative of physical prototyping, more computer techniques are being incorporated to visualize and to test the functionality of a digital mock-up toward interactive virtual prototyping [8]. Botkin [9] conducted design study in which parametric modeling of automotive front structure concept that utilizes carbon fiber composite materials was only used as a convenient method to create the finite element model. Several researchers have studied the optimization of performance of disc brake by the Taguchi's method of Design of experiments (DOE) to reduce the computational effort without affecting the final solution quality. Makrahy et al. [10] analyzed the disc brake using brake dynamometer and used Taguchi approach for DOE. Singh et al. [11] conducted optimized process parameters in order to study Performance of Brake Pads Using Taguchi's approach. Bhat and Lee [12] studied experimentally three ventilation parameters of the disc brake rotor using Taguchi method. Botkin [13] provided design methodology of Carbon Fibre Reinforced Composite Automotive Roof, including finite element analysis for realistic loading conditions, for specific major body component. Kothawade et al. [14] conducted numerical simulation using CFD analysis, in order to find the variations of the thermal transfer coefficients (h) during braking of the vehicle for each rotor area in order to exploit them in the search for the temperature reached in both disc designs (full and ventilated) while adapting the finite element method (FEM). The numerical solution of the resulting equations of the fluid–structure interaction problem poses great challenges since it includes the features of structural mechanics, fluid dynamics and their coupling [15]. These interactions can be physical, sensorial and cognitive [16] and are direct (they associate the system and an element of the environment) or indirect (they link two elements of the environment). García et al. [17] performed CFD simulation of complex phenomena in batch mode on large high performance computing (HPC) systems. Cucinotta et al. [18] investigated, with a preliminary numerical study by means of Computational Fluid Dynamics (CFD), Air Cavity Ships technology.

In work done by Tang et al. [19], and in the context of improving the accuracy of coupled computation techniques (CFD and FEM), modeling of the transient thermal transfer of brake disc was presented by the authors. To better understand this procedure, several parameters involved here, were addressed by them, such as, material, the type of braking and the geometry of the brake disc. Carfagni et al. [20] develop a numerical tool (CAD/FEM) to assist the designer willing to take comfort into account as a primary requirement for saddle design. Adamowicz and Grzes [21] used the finite element technique (FEM) in their study, to clarify the effect of the convection transfer coefficient (h) around the full disc during its heat dissipation phase. Ishak et al. [22] developed one dimensional (1D) model of leading-trailing drum-type parking brake model and then verified with experiments test bench. Belhocine and Nouby [23] developed finite element model of the whole disc brake assembly and validated by using experimental modal analysis. Etkins et al. [24] presented a PIV flow measurement of air flow in the ventilation channels thus cooling the disc down during braking operations. Zhang et al. [25] simulated the temperature change of the sinusoidal surface milling process by using the three-dimensional modelling software, Matlab and finite element analysis software. Devanuri [26] conducted numerical investigation using, RNG k–ε turbulence model, in order to examine the effect of an air brake on the aerodynamics of a ground, vehicle, and in addition, for the study the influence of certain parameters such as the inclination angle, the vehicle velocity, altitude and the position of the air brake on the aerodynamics of the vehicle body.

The main purpose of this scientific contribution is to present numerical simulation during stop braking step in order to visualize the thermomechanical behavior of the automobile brake discs while considering the generation of initial heat flow generated by friction between both parts in dry contact (the rotor and the brake pads). In this interactive approach, we have developed a numerical solution based on the finite element method. The method is applied to mechanical design for automotive braking system. The interactive character is present through the consideration of interactions (thermal, tribological and mechanical). We focused first, our intelligence on the actual evaluation of the values of convective Heat Transfer Coefficients (HTC) as function of time, by adopting the ANSYS CFX code of which these, have been used in the prediction of the transient temperatures of brake discs while seeing the performance of three gray cast

irons. So we have detailed the problem of degradation of the vehicle brake discs by thermal fatigue. Fatigue phenomena, which appear generally below the yield stress is the cause of more than 80% of in-service mechanical failures [27].

Our general concern here is to identify the disc material that is more tolerant to temperature increases. Thus, comparative results on temperatures of the two discs allowed us to get the best cooling style that is used in the prototype of manufacture of automotive brake discs. These results are quite in good agreement with those found in reality in the brake discs in service and those that may be encountered before in literature research investigations of which these are very useful for engineers and in the design field in the vehicle brake system industry. These are then compared with experimental results obtained from literatures that measured ventilated discs surface temperatures to validate the accuracy of the results from this simulation model. This work also aims to perform a coupled thermomechanical analysis under the ANSYS Multiphysics to simulate the behavior of a brake disc in contact with the brake pads. This simulation allowed us to visualize some important results such as, the global deformations and the constraints of Von Mises stress of the model (disc-pads), the contact pressure distribution of the inner pads as well as, the influence of the grooved brake pad and the mode of loading exerted by the piston on the stresses established on the structure. We finally compared these numerical results with experimental results obtained from literature containing measurements of ventilated discs surface temperatures to validate the accuracy of the results from this simulation model. The results of this analysis are in accordance with reality and the current life of the braking phenomenon and the brake discs in service thus with the thermal gradients and the phenomena of damage observed on used discs brake.

2 Disc brake system and operation

Brake rotor is defined as any metal part generally mounted on wheels of the vehicle before the braking process, and planted to brake pads inside fixed caliper composed of piston constituting two elements; filling or friction material and sheet steel base (Figure 1).

3 Brake disc kinds

We know in the field of the automobile, two kinds of brake discs; full discs and ventilated discs. Full discs usually have crown attached to bowl disc which is nailed to the wheel of the vehicle (Fig. 1a).

Ventilated brake discs are modern discs of complex shape used in our time when they are equipped with front

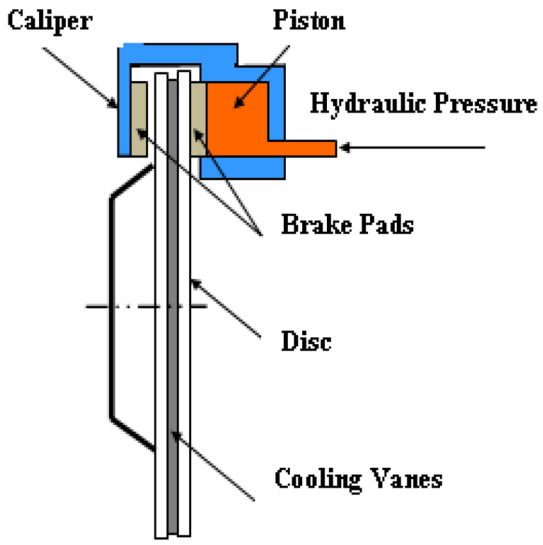

Fig. 1 The composition of braking system

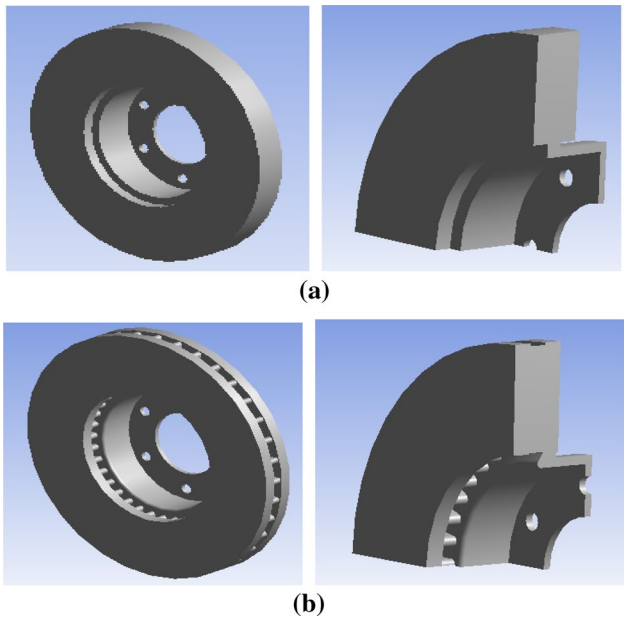

Fig. 2 CAD model of discs brakes: **a** Full disc. **b** Ventilated disc

axles of vehicles by constituting two so-called broken crowns which are separated by fins (Fig. 2b). In geometric design of the ventilated brake discs, these fins provide good cooling and excellent ventilation compared to full discs by raising the area of the convective heat exchange. Taking into account the variation of elements to know; the material, the size and the geometry of the fins (circular pins, curves, radial fins), the ventilated discs are completely constructed thus guaranteeing good thermal absorption capacity.

But Etkins et al. [24] showed that the rotation of the disc is capable of inducing air flow through the slots to increase the cooling rate of the brake disc.

4 Research methodology

A simulation methodology has been developed in order to investigate coupling thermomechanical analysis of disc brake assembly. Nowadays, most of the simulation models are implemented with the finite element method [28]. The CFD code was used to calculate convective heat transfer coefficients on the surfaces of the parts involved in the coupling process as well as the air temperatures next to the surfaces. These are the values required to compute convective heat transfer from the surfaces of different parts. In reality, the process is somewhat more complicated, since the convective heat fluxes are changing with time and should not be considered constant. The overall simulation methodology is divided into three main steps:

- CFD Analysis performed under ANSYS-CFX in order to calculate the values of heat transfer coefficients (HTC) for each surface of the disc brake. Because heat transfer coefficients (HTC's) are dependent on temperature, it was necessary to couple the CFD and FEA solutions.
- Thermal analysis under ANSYS Workbench in order to calculate the temperature distribution of the disc brake rotor using the FEA model.
- Structural analysis under ANSYS Workbench of which it is advisable to resort to a weak coupling resolution consisting of first determining the temperature field independently of the mechanical conditions and then evaluating the stresses and deformations induced by this field temperature.

The developed approach and general methodology adopted for performing thermo-structural analysis of a disc brake rotor can be explained by following flowchart shown in Fig. 3.

5 CFD modelling and analysis with ANSYS CFX

Any solution of nonlinear partial differential equations describing turbulence problems, fluid motion and heat transfer phenomena as well as; vehicles aerodynamics problem is essentially based on the procedure of the computational fluid dynamics (CFD) by means of computer-based simulations. This technique is very powerful and currently widely used in industrial and non-industrial applications. This numerical technique is based on the resolution of transport equations written in a conservative form [29]. However, despite technological and computer developments, CFD calculations remain expensive in terms of both resources and time [30]. With precise solution of these equations using this adopted procedure, fast and reliable convergence can be achieved while estimating the physical parameters of the fluid flow as; speed, temperature, viscosity, and pressure.

5.1 Solution procedure of CFD analysis

ANSYS CFX software is high-performance advanced resolution technology used especially in the field of computational fluid dynamics, as large flow solution application, it allows us to provide highly accurate, reliable, robust and fast solution results. ANSYS CFX consists of three modules that communicate with each other as shown in Figs. 4 and 5. Software that allows the realization of geometry and mesh is required for performs a CFD analysis.

5.2 Governing equations

In this analysis, we presented a simplified model and simulation of surface heat flux in the brake disc caused by friction while using ANSYS CFX software. The model that was discussed here in this study is similar to that developed by Palmer et al. [31]. All equations used in CFD analysis, namely, the Navier–Stokes moment equation, the energy equation, and the continuity equation were used to solve the thermal problem, which is the variation of heat transfer and air flow around the brake disc.

(a) Continuity Equation

The mass conservation equation in the case of compressible and incompressible flows is defined as follows

$$\frac{\partial \rho}{\partial t} + \nabla.(\rho u) = S_m \tag{1}$$

where S_m is the mass added to the continuous phase from the dispersed second phase.

(b) Momentum (Navier–Stokes) Equations

In inertial frame, the governing momentum conservation equation is given by the form:

$$\frac{\partial (\rho v)}{\partial t} + \nabla.(v\, v) = -\nabla p + \nabla.(\tau) + \rho g + F \tag{2}$$

where the stress tensor τ is of the form:

$$\tau = \pm\mu \left[(\nabla v + \nabla v^T) - \frac{2}{3} \nabla.v I \right] \tag{3}$$

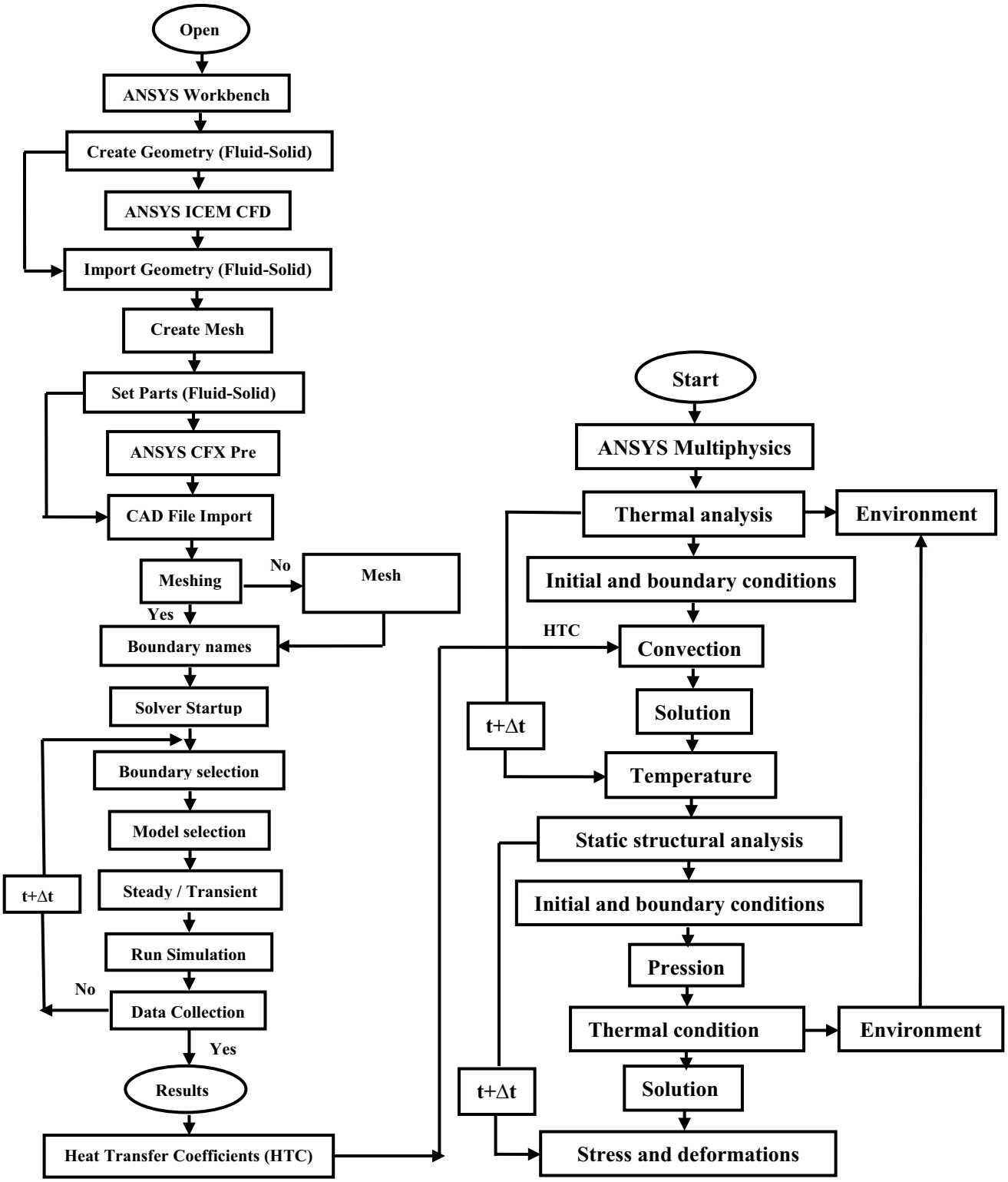

Fig. 3 Flowchart for the developed approach based on ANSYS thermos-mechanical simulation

The left term of Eq. (2), can be reduced to the form below by using the rotating reference frame (RRF) technique in the case of rotating brake disc and in absolute velocity.

$$\frac{\partial(\rho v)}{\partial t} + \nabla.(\rho v_r v) + \rho(\Omega \times v) \tag{4}$$

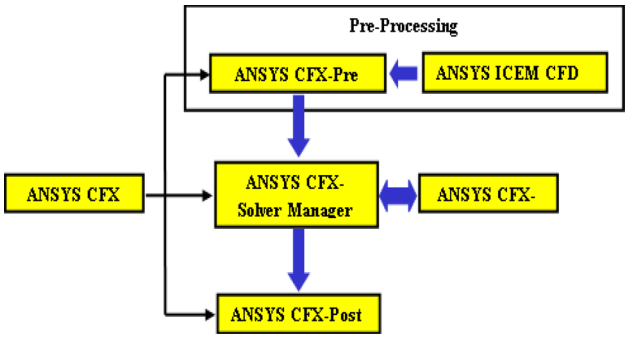

Fig. 4 ANSYS CFX code structure

where Ω and v_r are respectively, the angular velocity and the absolute velocity, the continuity equation used in analysis (RRF) is expressed;

$$\frac{\partial \rho}{\partial t} + \nabla \cdot (\rho v_r) = S_m \tag{5}$$

5.3 Heat flux entering the disc

During active braking process of moving vehicle, its kinetic energy is converted to heat energy by dry friction between the two parts (disc and brake pads) producing a distribution of heat flux on both sides of the disc. The general formula for calculating the initial flux entering the automotive brake disc can be expressed as follows [32]:

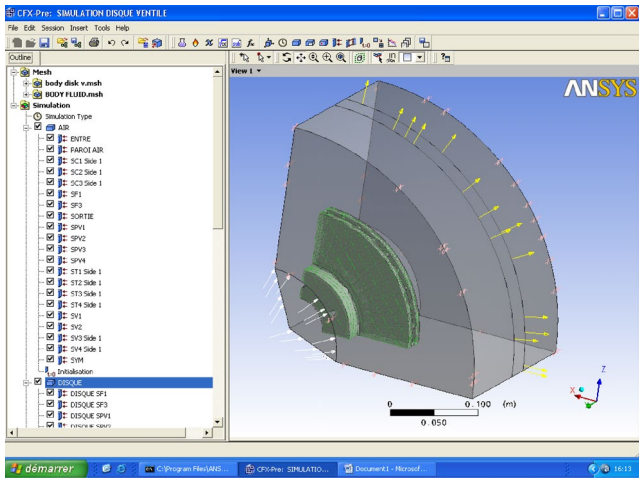

(a) CFX Pre module.

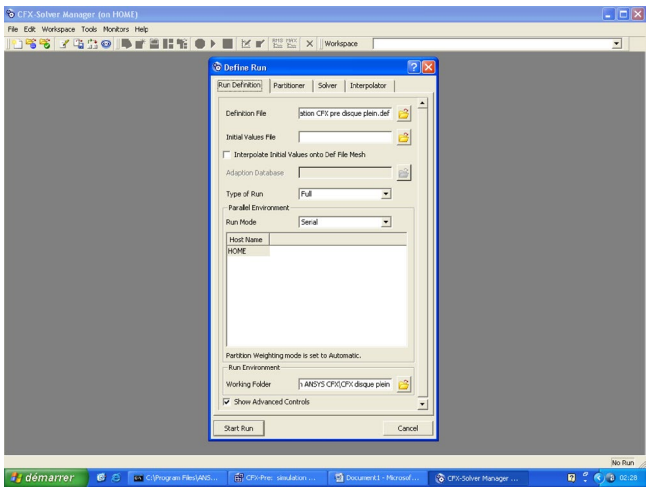

(b) ANSYS CFX-Solver Manager module.

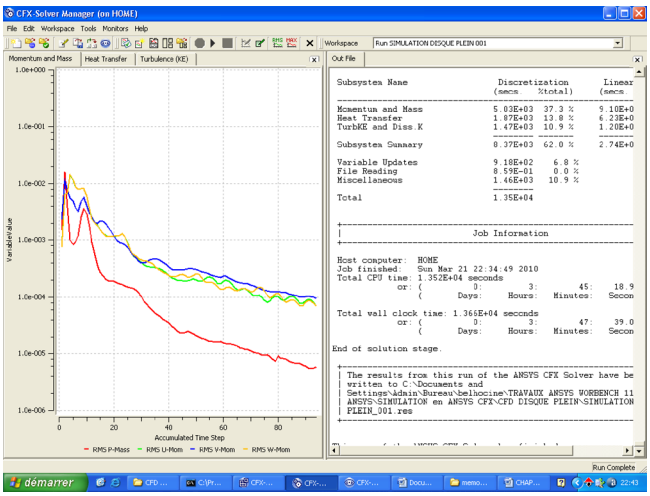

(c) ANSYS CFX-Solver module.

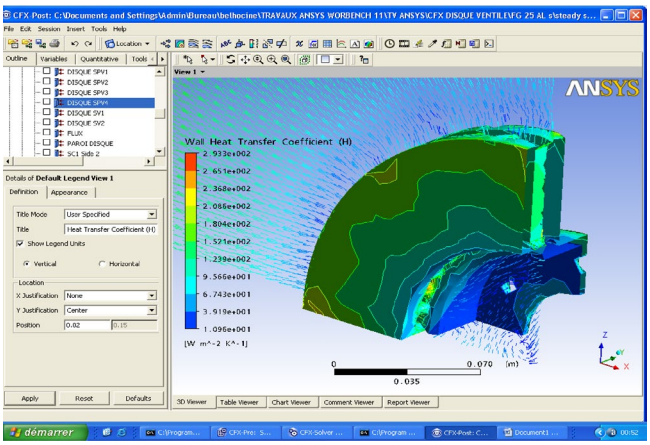

(d) ANSYS CFX-Post module.

Fig. 5 Calculation progress with ANSYS CFX

$$q_0 = \frac{1-\varphi}{2}\,\frac{m\,g\,v_0 z}{2\,A_d\,\varepsilon_p} \tag{6}$$

where, g is the acceleration of gravity (9.81) [ms^{-2}], a is the vehicle deceleration [ms^{-2}], $z = a/g$ is the braking efficiency.

The quantity evaluated using Eq. (6) of the initial heat flux has been exploited of course in first step of the CFD analysis, and then, in transient thermal analysis using finite element software ANSY Workbench 11.0 to visualize the variation of the brake disc temperature.

In this contribution, we evaluated the transient values of the heat transfer coefficient (HTC) by using ANSYS-CFX software, which has been substituted in Multiphysics analysis to predict the three-dimensional temperature (3D) of the brake disc. In fact, this latter absorbs an amount of more than 90% of the thermal energy generated by friction [33]. Given the complexity of the phenomenon treated, we assumed that the thermal flux entering the rotor, and the brake pads replace the effect of dry friction between the two bodies in contact, as shown in Fig. 6.

The heat flux generated in the rotor area is considered a thermal loading. In our scientific contribution, we used ventilated brake disc made of high-carbon gray cast iron material FG, whose disc having the geometric dimensions (262 × 29 mm) equipping certain types of vehicles (Fig. 7).

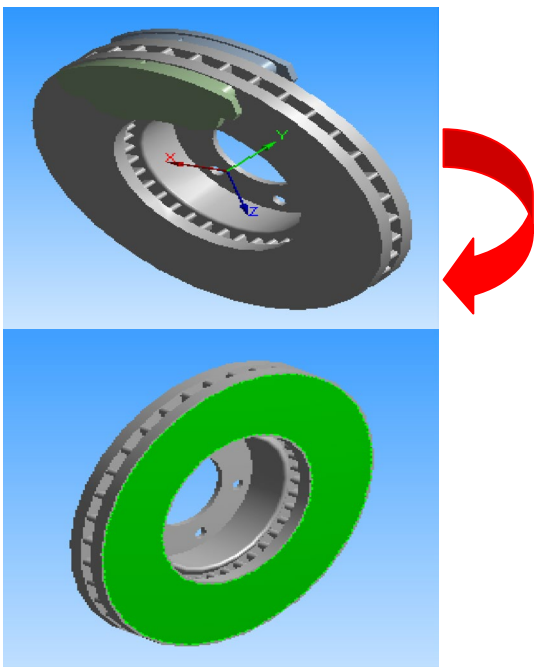

Fig. 6 Heat flux from braking friction

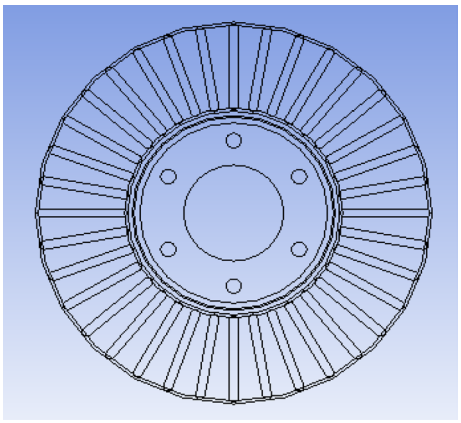

Fig. 7 Contour view of ventilated disc

5.4 k–ε turbulent model

The turbulence model (k–ε) is the most widely used model in the field of CFD analysis as numerical simulation of the average flow characteristics in the turbulent flow regime. It is two-equation model that gives general description of turbulence using two partial differential equations (PDE) called the transport equations, one for turbulent kinetic energy (k) and other for dissipation (ε). For current models, the model provides a good agreement for accuracy and virility.

5.5 Modelling assumptions

In order to facilitate CFD calculations, we have introduced the assumptions that are summarized as:

- The flow medium is air
- The vehicle starts with initial speed of 28 m/s,
- The pure nature of the fluid in calculation is air,
- The air inlet speed is fixed at 28 m/s
- The regime is steady-state turbulent incompressible flow around the disc brake rotor according to the turbulence model k–ε.
- The thermo-physical properties taken into account in the calculation are constant like (viscosity, specific heat, thermal conductivity, and density).
- The radiation phenomenon is neglected whereas only conduction and thermal convection are considered here.
- The distribution of heat flux on area of the brake disc is quite uniform
- Under normal pressure and temperature conditions, the physical properties of the air are considered
- Heat Flux is uniform over pad area.
- Brake disc absorbs almost 90% of thermal friction

5.6 CFD analysis with ANSYS CFX

In studies, much attention was paid to characteristics and complex nature of the flow around the rotating disc (s), whether it be laminar, regular swirling, axisymmetric, or thermal transfer [34, 35]. Knowledge of the coefficient of exchange (h) in the flows is important and in the large backwater simulation, the renormalization group (RNG) k–ε turbulence model is usually considered desirable choice regarding rotation or swirling flow.

Various external and internal faces of the two structures, full and ventilated disc that were derived from the code ANSYS ICEM CFD are shown in Figs. 8 and 9.

Finite volume method is common approach used in the ANSYS CFX codes is essentially based on the elements to which the discretization according to mesh of the spatial domain gives us finite volumes that are exploited for the conservation of the high quantities namely, the energy, mass and momentum. Mesh normally in CFX is in three dimensions, nevertheless in order to simplify things; this one has been demonstrated only in double dimensions.

The mesh is realized here, in linear tetrahedral elements with 179798 elements and 30717 nodes (Fig. 10). ANSYS-CFX code solves the CFD aerodynamic model of the brake disc while basing on transitory type of the problem whose all boundary conditions were injected in both domains (solid and fluid).

In this study, we have considered that the ambient air temperature at 20 °C surrounding the brake disc is equal to it in the initial state, zero relative pressure of which has been maintained at the high, low and radial edges of the fluid domain.

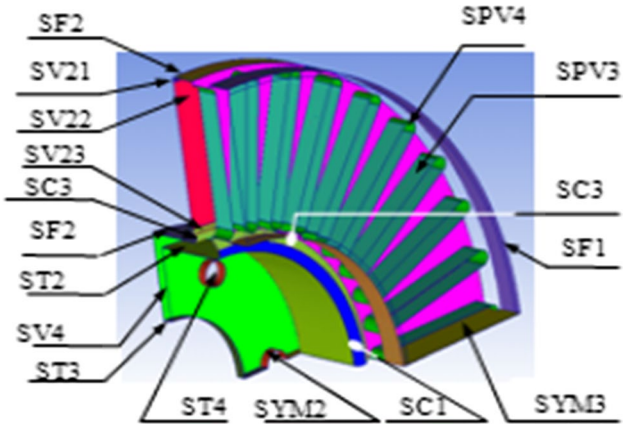

Fig. 9 Quarter of the ventilated disc showing the assignment of face names

5.7 Fluid mesh generation

In this study, the size of the fluid body is 1.95 e-7 $mm^{3,}$ and the mesh generated on the model characterizing the fluid domain is tetrahedral mesh containing 179798 elements, and 30717 nodes, as shown in Fig. 11.

Actually, ventilated brake disc consists of two full discs connected to each other internally by fins that form tunnels with open side for the passage of air to flow from the inside diameter and out to the outer diameter of the disc. Centrifugal force due to disc rotation, forces the air in the channels to flow outwards to the perimeter of the disc. This creates a continuous flow of air from the access zone and exits from outside to ambient air in the area called air outlet area. Due

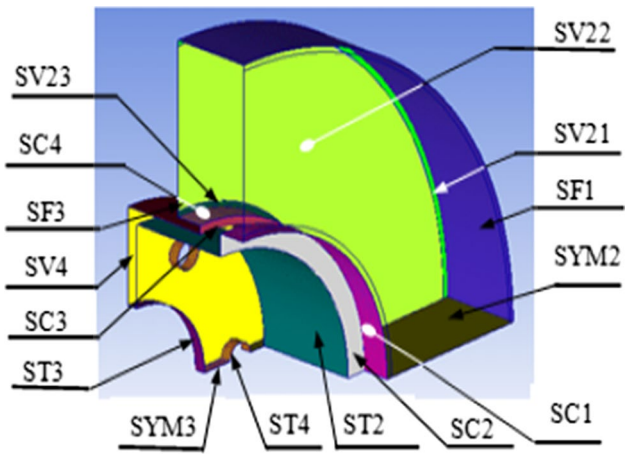

Fig. 8 Quarter of full disc showing the assignment of face names in the simulation

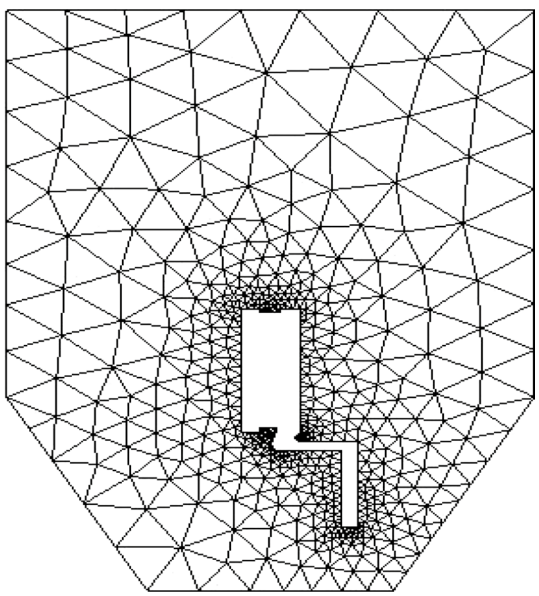

Fig. 10 Wall meshes for the CFD simulation

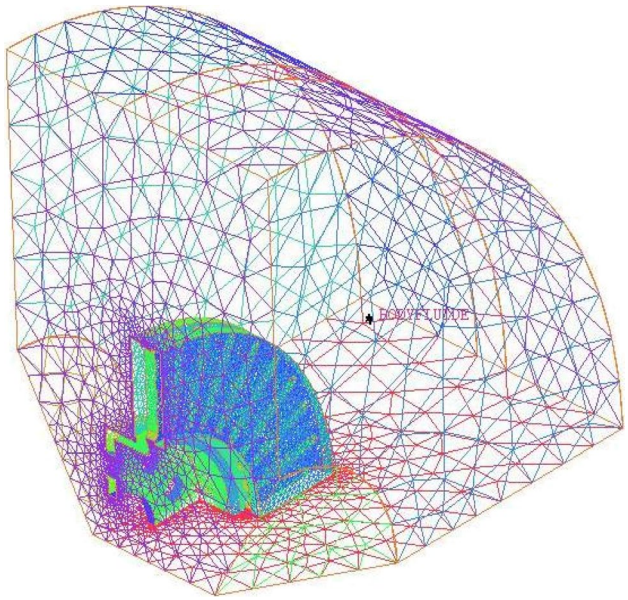

Fig. 11 Meshing for a fluid body

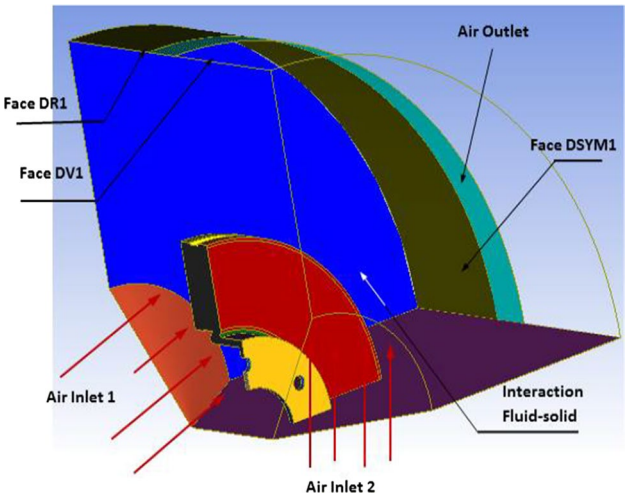

Fig. 12 Fluid body surfaces in ANSYS ICEM CFD

to symmetrical shape of the brake disc, we modeled only quarter of the fluid domain geometry using ANSYS ICEM CFD software which gives us the graphical interface shown in Fig. 12.

5.8 Boundary conditions and computational details

When the model for every element is defined, all the physical parameters (variables, values, initial and boundary conditions) are determined for the braking system design. Any simulation on ANSYS software for its version ANSYS Mechanical or Multiphysics makes it possible to define database or materials properties that characterize the elements to be analyzed. These, are integrated directly from ANSYS Workbench into the materials library taken at air temperature at 20 °C before any preliminary step. In the present study, we have selected three types of gray cast iron materials used in the design of brake discs to study their performance, in this case, gray cast irons (FG25AL, FG20, and FG15). Disc brakes must withstand very strong mechanical and thermal stresses in performing its stopping duty.

High carbon fires are also the most commonly used materials in the automotive industry because of their advantageous thermal and tribomechanical properties. The strength and hardness of ferrite are greater in cast iron than in steel due to the hardening effect of silicon. Cast irons have compressive strength 3–4 times higher than their tensile strength. We introduced the temporal conditions of the simulation of the braking process in ANSYS Workbench platform taking 3.5 s as the braking time to time step increments of 0.01 s.

In this calculation, given the symmetry of the disc and the periodic repetition due to rotation of the rotor, the entire model of the disc is reduced and simplified to only a quarter to reduce the calculation time for simulation, that is why the conditions boundary, periodic and symmetrical have been so designated.

In order to easily model the rotational aspect of the automobile brake disc in the environment, the output and inlet edges of the fluid model are maintained in atmospheric temperature and pressure. The surrounding air temperature of the disc is set at 20 °C using rotating reference frame for the management of the moving brake disc. Symmetrical boundary conditions are also used to produce shear walls with zero shears. CFD model developed in ANSYS CFX used in search for exchange coefficient values (h) is well shown in Fig. 13.

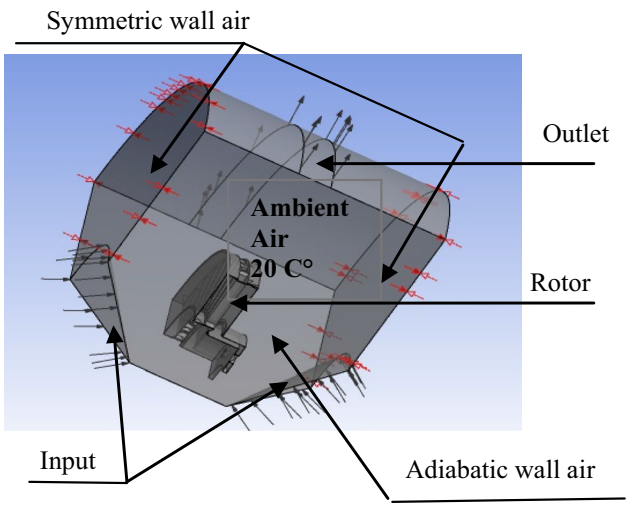

Fig. 13 CFD model of ventilated disc brake

6 Finite-element modelling

Finite element method (FEM) consists of approaching, in a finite-dimensional subspace, problem written in variation form (as minimization of energy, in general) in infinite dimensional space. The approximate solution is in this case, is function determined by a finite number of parameters such as, for example, its values at certain point (the mesh nodes). Its advantages lie mainly in possible treatment of complex geometry, more natural determination of boundary conditions, the possibility of mathematical convergence demonstrations, and error enhancement. On the other hand, its disadvantages sum up in complexity of the implementation and cost of computing time and in memory. However, for real problems involving complex material properties and boundary conditions, a numerical method of analysis is more suitable. The most popular of the various numerical methods that have been developed is the finite element (FE) method. Two types of FE analysis are widely used in brake design: heat transfer analysis to determine transient temperature distributions and thermal stress analysis to determine stresses and strains due to these non-uniform temperature distributions.

6.1 Modelling assumptions

The standard dimensions of the full and ventilated brake disc are identical in this numerical simulation to ensure a better comparison of the results. Table 1 lists all the physical parameters and the geometric dimensions of the brake disc used in numerical calculations.

The material of the brake disc that we have opted for in this simulation, having carbonaceous assembly is gray cast iron (FG15) [36], having excellent tribological and thermo-mechanical properties. We consider that brake pads having a material characterized by purely isotropic elastic behavior whose properties of the two parts involved are explained in Table 2 below.

Table 1 Design parameters of brake disc

Parameter	Value
Inside diameter of the disc, mm	66
Outside diameter of the disc, mm	262
Disc thickness (TH), mm	29
Disc height (H), mm	51
Weight of the car m, kg	1385
Initial velocity v_0, m/s	28
Deceleration a, m/s^2	8
Time of braking t_b, s	3.5
Effective disc radius $R_{disc,}$mm	100.5
Ratio braking forces distribution ϕ, %	20
Factor of disc charge distribution ε_p	0.5
Disc's swept area A_d, mm^2	35993

Table 2 Properties of the disc and pad

Material properties	Disc	Pad
Thermal conductivity, k (W/m °C)	57	5
Volumetric mass density, ρ (kg/m^3)	7250	1400
Specific heat capacity, c (J/Kg. °C)	460	1000
Poisson's ratio,	0.28	0.25
Friction coefficient, μ	0.2	0.2
Young modulus, E (GPa)	138	1

Research investigations showed the difficulty of to actually model rotating brake disc, due to simultaneous interaction of several tribological and vibro-thermomechanical phenomena during automotive braking. Nevertheless, these tips can be solved numerically and in approximate way on the basis of certain reducing hypotheses, allowing solving these problems quickly. Series of reasoning hypotheses have been applied here, throughout the duration of the braking [37]. These assumptions which are made while modeling the process are given below:

- In this simulation, two modes of heat transfer by conduction and convection are considerable in internal and external faces of the brake disc in such way that the radiation exchanges are negligible [38].
- The kinetic energy of the vehicle which is dissipated during the braking mechanism is totally converted into heat energy represented by a heat flux distributed on the faces of the brake disc.
- The kinetic energy of the vehicle is lost through the brake discs i.e. no heat loss between the tire and the road surface and deceleration is uniform.
- The initial temperature of the disc is constant and is equal to the air temperature of the environment at 20 °C
- The physical properties of the brake disc material are isotropic and homogeneous and their thermal properties are dependent on temperature.
- During the braking time, the inertia and all other forces are considered negligible
- The domain is considered as axis-symmetric
- Brake distribution is 60% on front, 40% on rear
- Force distributed on one brake disc in is equal the total frictional force applied on rubbing surface
- Before the braking phase, the brake disc is free of any stress
- All parts of the brake disc are subject to the phenomenon of thermal convection such as; the outer ring diameter area, the outer ring diameter area, the cooling fins, and the disc brake surface

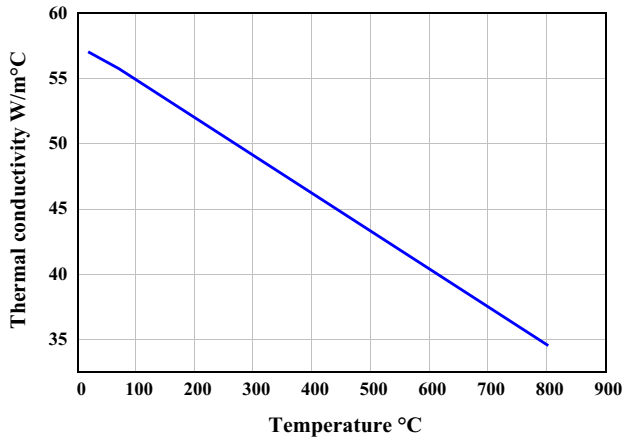

Fig. 14 Thermal conductivity versus temperature

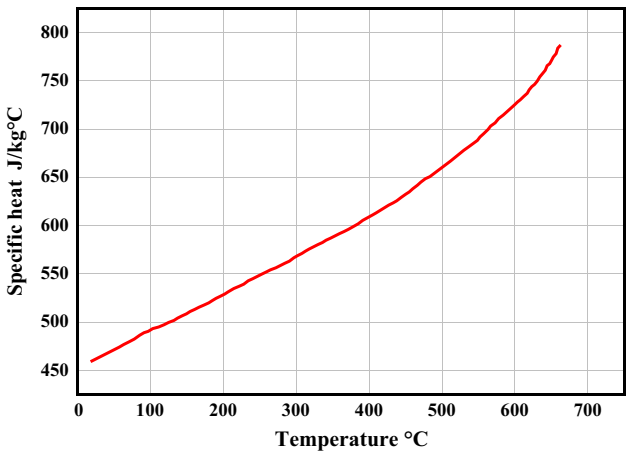

Fig. 15 Specific heat capacity versus temperature

Conductivity as well as the specific heat capacity of the brake disc material; are varied with temperature as shown in Figs. 14 and 15.

6.2 Auxiliary equations

The general three-dimensional heat transfer equation in isotropic material in Ω domain is given as follows

$$-\left(\frac{\partial q_x}{\partial x}+\frac{\partial q_y}{\partial y}+\frac{\partial q_z}{\partial z}\right)+Q=\rho c\frac{\partial T}{\partial t}dxdydz \tag{7}$$

where T (x, y, z, t) is the temperature field, ρ is the density, C, is the heat capacity, $Q=Q\ (x,\ y,\ z,\ t)$ is the internal thermal energy by unit of volume, q_x, q_y and q_z are respectively the surface heat flux units along the x, y and z directions,We can define like this, the thermal fluxes according to the directions of the axes x, y and z according to the Fourier law:

$$\begin{cases} q_x = -k\dfrac{\partial T}{\partial x} \\ q_y = -k\dfrac{\partial T}{\partial y} \\ q_z = -k\dfrac{\partial T}{\partial z} \end{cases} \tag{8}$$

where k is the thermal conductivity. By substituting Eq. (8) in Eq. (7), we obtain the following differential equation, which varies as function of temperature T

$$\frac{\partial}{\partial x}\left(k\frac{\partial T}{\partial x}\right)+\frac{\partial}{\partial y}\left(k\frac{\partial T}{\partial y}\right)+\frac{\partial}{\partial z}\left(k\frac{\partial T}{\partial z}\right)+Q+\rho c\frac{\partial T}{\partial t}dxdydz=0 \tag{9}$$

The boundary conditions imposed on our thermal problem are expressed as follows:

- Temperature of fluid that enters the domain is based on the value specified temperature

$$T_S=T_1(x,y,z,t)\quad on\quad S_1 \tag{10}$$

- Heat flux is controlled by the temperature gradient and always flows from high temperature regions to lower temperature regions.

$$q_x n_x+q_y n_y+q_z n_z=-q_s\ on\quad S_2 \tag{11}$$

- Convection is group of thermal boundary conditions in which heat flow is a function of convection

$$q_x n_x+q_y n_y+q_z n_z=-h\ (T_s-T_e)\ on\quad S_3 \tag{12}$$

where h is the convective exchange coefficient; T_e is the convection surface temperature, and T_s is temperature unknown to the S area. Knowledge of the initial temperature field at the time ($t=0$) for any transient modeling is mandatory.

$$T(x,y,z,0)=T_0(x,y,z) \tag{13}$$

6.3 Thermal loading applied to the disc

In this research work, we carried out numerical modeling of the transient thermal transfer in disc brake, by finite element method in which the type of braking of the adopted vehicle is that of emergency stop braking. The speed of the vehicle decreases linearly as a function of time until the moment of braking (t = 3.5 s), stabilizing at the value zero until the end of this braking at the instant (t = 45 s), as shown in Fig. 16.

The heat flux is identified here as the thermal load which is generated by dry friction between the brake disc and the pads during the braking phase. At first, the value

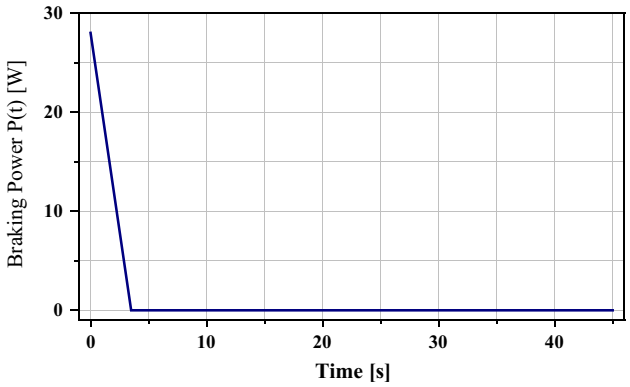

Fig. 16 Braking power versus time

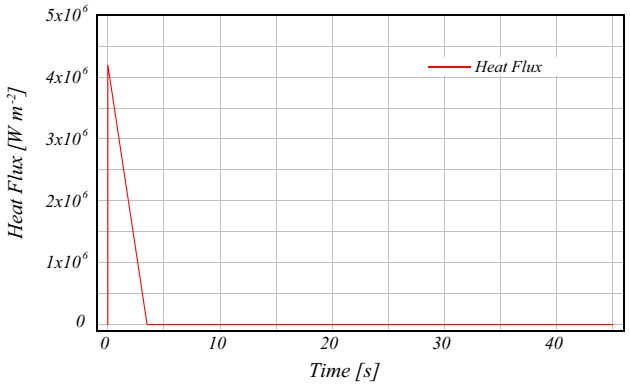

Fig. 17 Heat flux versus time

of this flow is maximum and it then decreases linearly until it vanishes at the end, as shown in Fig. 17.

6.4 Mesh of disc brake model

The application of generated mesh of brake disc in numerical modeling is useful from which one has chosen automatic mesh generation. It should be kept in mind that mesh too fine will require very long calculation times and thus increase the final cost to the engineer. Taking into account all this, a fine mesh was chosen to visualize the variations of temperature and heat flow. Thus, the results obtained are more precise. On both brake disc friction tracks where the brake pads are turning, refined tetrahedral mesh has been performed on the ANSYS Multiphysics.

The final mesh therefore, comprises 172103 nodes and 114421 elements for the full disc, and 154679 nodes and 94117 elements for the ventilated disc, as it is represented in Fig. 18.

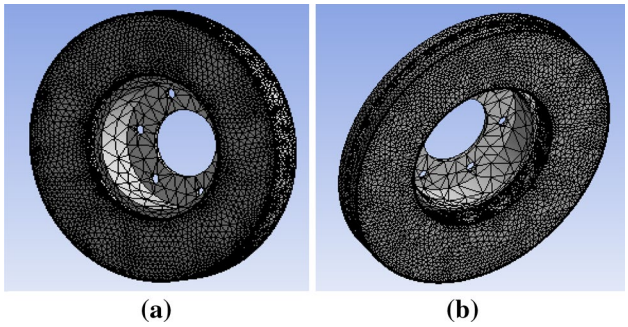

Fig. 18 Disc brake mesh model: **a** Full disc. **b** Ventilated disc

6.5 Boundary conditions applied to the model

As thermal analysis is done, the conditions to be taken into account are those that will influence the thermal phenomena such as ambient temperature and that of the fluid. The objective of this study is to perform thermal analysis of brake disc using the ANSYS Workbench software, while selecting transient thermal analysis mode by injecting all the thermo-mechanical properties of the materials used in the analysis, such as the disc and the brake pads. We introduce the associated boundary conditions for each disc area.

Modeling requires discretization of the time axis. Unlike numerical control, the discretization of the time axis does not have to be regular. The parameters of the initial, minimum and maximum and final time increment for the simulation shall be inserted at the values (0.25 s, 0.125 s, 0.5 s, 45 s) respectively, maintaining the initial temperature of the disc at 20 °C. The thermophysical characteristics of the 3 types of gray cast iron brake discs (FG 15, FG20, and FG25AL) are introduced in the simulation. The values of the convection exchange coefficient (h) for each face of the brake disc must be imported from CFX analysis results and must be used in the ANSYS Workbench Multiphysics analysis. These are shown in the following in the graphs of Fig. 27a, b. The imposed heat flux on the lateral surfaces corresponds to their values resulting from the CFX analysis.

6.6 Solution procedure of FE analysis

ANSYS Workbench is a powerful platform that allows you to perform all the steps of the simulation using the finite element method in single interface and to connect the different modules and associated physics (fluids, thermal, structure…). The direct interfacing of ANSYS Workbench with CAD makes it possible to transfer the geometries without risk of errors and to take full advantage of the synergy between the simulation software and the CAD before access to the ANSYS Design Modeler, and the ANSYS Multiphysics (Figs. 19 and 20).

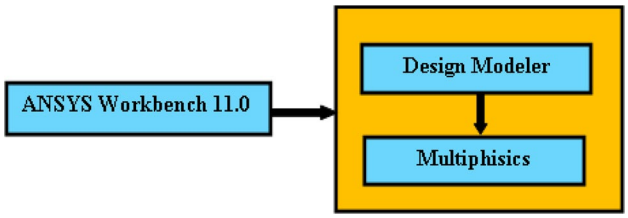

Fig. 19 ANSYS Workbench 11 module

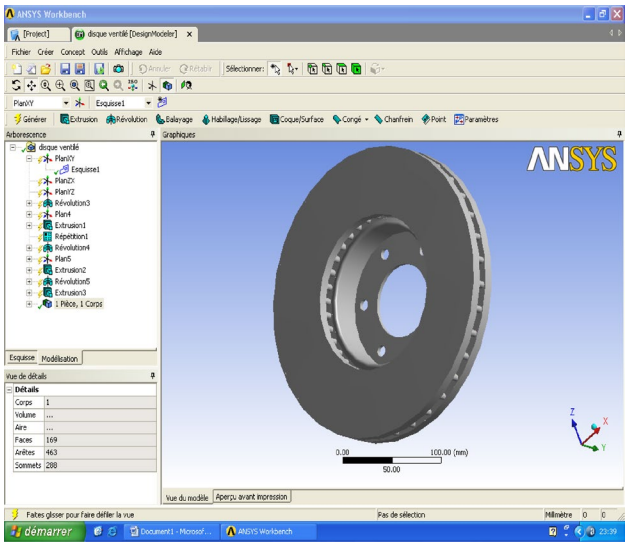

(a) Design Modeler module.

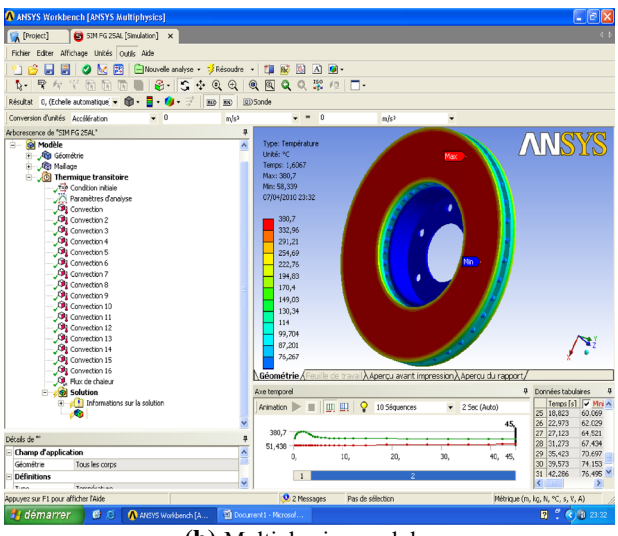

(b) Multiphysics module.

Fig. 20 ANSYS Workbench 11 modules

7 Experimental setup

The numerical results of the thermal simulation obtained in this work using ANSYS, are validated using the results of the work of Stephens [39], which was an experimental investigation on temperature distribution of ventilated disc brake rotor.

7.1 Temperature measuring with embedded thermocouple

The temperature measurement was conducted using Cu thermocouples integrated in the disc brake rotors according to VDA285-1, which became accredited until the year 1996, at the mean friction radius as shown in Fig. 21a. The temperature pot-side was measured also by Cu-embedded thermocouple as shown in Fig. 21b. The thermocouples have a cylindrical shape in this case with the sizes Ø = 3 mm and h = 3 mm as in Fig. 21c. The connecting wires were insulated on the brake-rotor-side and were connected to the signal amplifier.

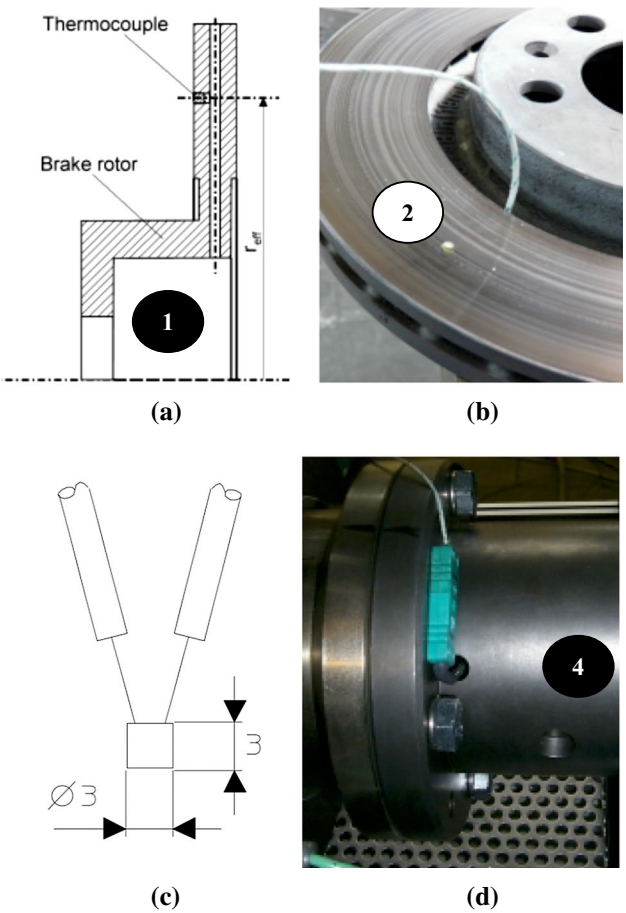

Fig. 21 Temperature measuring with embedded thermocouple as per VDA285-1

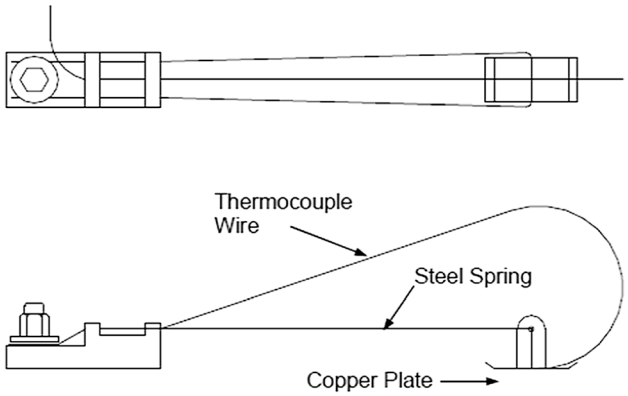

Fig. 22 Diagram of disc brake thermocouple

7.2 Disc brake thermocouples

Thermocouples are the favored choice for testers due to their cost, ease of use and availability, and are one of the most stable methods of measuring the temperature of disc brakes in vehicles with rubbing disc brakes. The device contains K-type thermocouple, which is made using silver wire welded to a flat piece of copper plate, and this plate is strongly supported against the rotating disc by steel spring. Elementary diagram of the thermocouple is provided in Fig. 22.

7.3 Experimental procedure

The brake was connected to the external applicator and the right rear wheel of the racing vehicle was fitted in the brake test rig as shown in Fig. 23. The rubbing thermocouple was positioned to measure the temperature on the inner surface of the rotor. The thermocouple data were recorded in the PC via a Fluke data logger.

The tests were performed by rotating the wheel at constant speed approximately equal the vehicle speed of 108 km/h. Progressive braking load was applied and the temperatures were recorded at very short intervals of 0.01 s. The method started with the disc heating up to temperature of about 345 °C, at which point the braking load was released. The recording continued there on until the temperature of the rotor dropped to about 200 °C. The results of the thermocouple readings were obtained directly from the PC in temperature scale.

8 Results and discussion of CFD analysis

8.1 Steady-state cases

The results obtained from the distribution of the wall heat transfer coefficient of the two brake discs in the steady-state case are illustrated in Figs. 24 and 25.

Table 3 lists the average heat transfer coefficients of the named surfaces in the CFD model of the full brake disc made of the material FG15.

The distribution of the heat transfer coefficient to the wall (h) according to the three types of brake disc materials is well represented in Fig. 25. It is observed that the variation of (h) in the brake disc does not subordinate to the material and that this one is not the same one found in the specialized literature.

From the maximum and minimum values of the various areas of the ventilated brake disc, the average values of the heat transfer coefficient can be taken from the wall (h). These harvested data are grouped in Table 4. From the

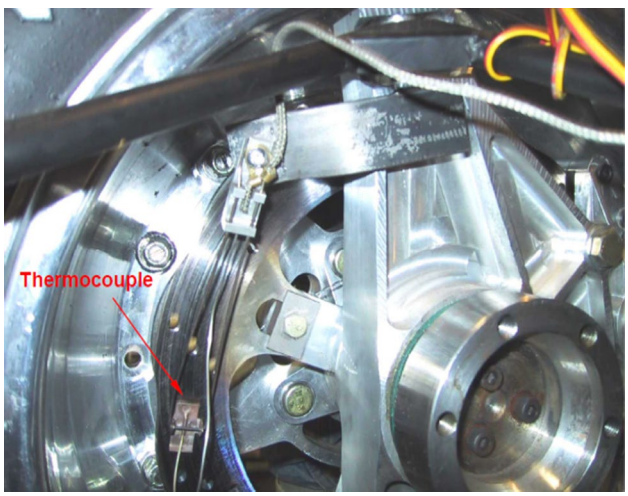

Fig. 23 Close up view of thermocouple in position

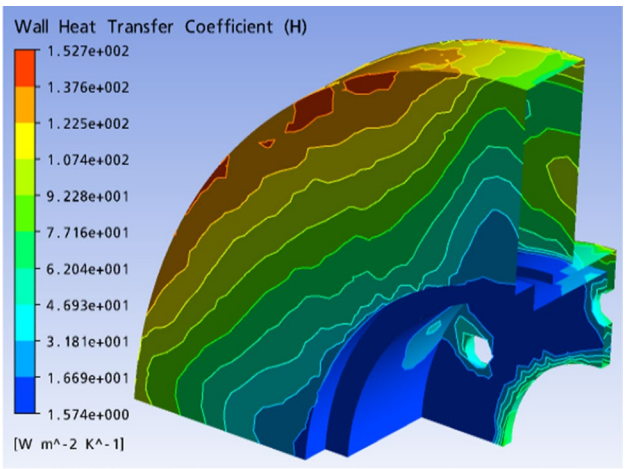

Fig. 24 Values of heat transfer coefficient at the wall of the full disc with material FG15 in steady state thermal analysis

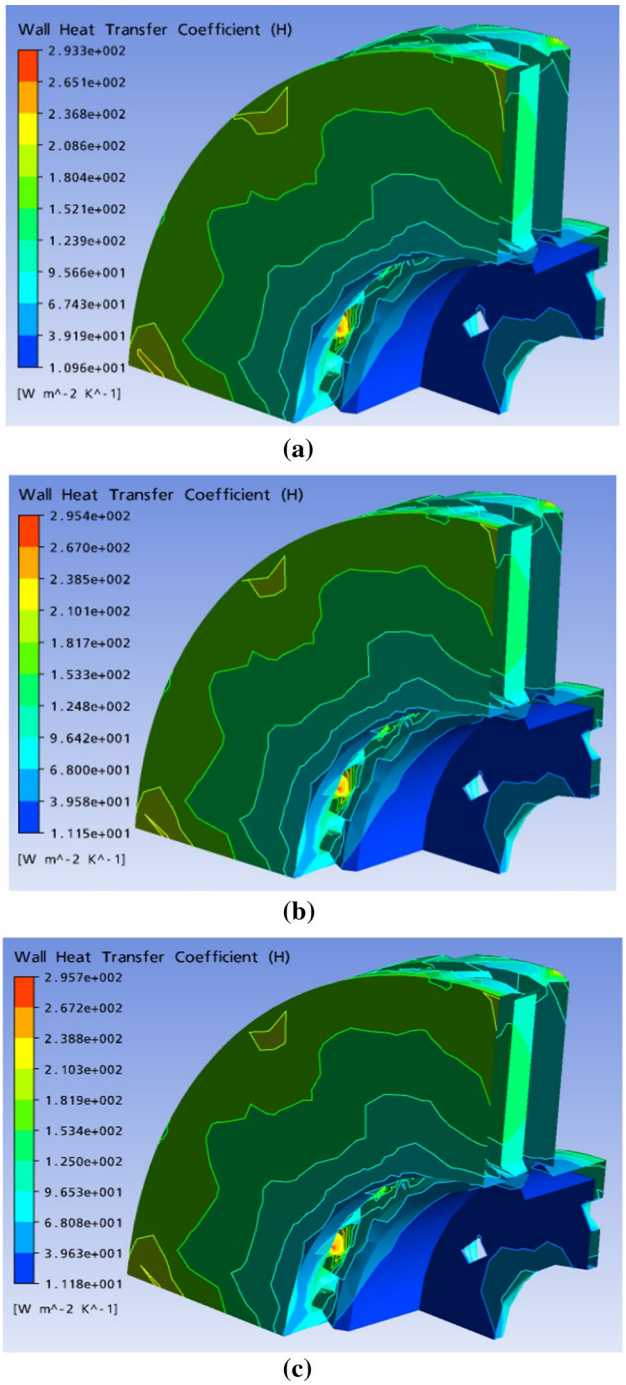

Fig. 25 Values of heat transfer coefficient at the wall of the ventilated discs with materials **a** FG25 AL, **b** FG20 and **c** FG15 in steady state thermal analysis

observation, it can be seen that there is no significant variation in this coefficient (h) when changing the material of the brake disc. Contrary to what we have seen, the heat transfer coefficient values at the wall are much more influenced by the ventilation system of the brake disc for the same material (FG15).

Table 3 Values of the wall heat transfer coefficients of different surfaces in the steady state case for full disc with material FG15

Surface	Material FG15 $h_{average} = [W\ m^{-2}\ k^{-1}]$
SC1	25.29168
SC2	5.18003
SC3	2.922075
SC4	11.77396
SF1	111.20765
SF3	53.15547
ST2	23.22845
ST3	65.6994
ST4	44.26725
SV1	81.37535
SV2	71.75842
SV3	41.83303
SV4	65.82545

Table 4 Values of the wall heat transfer coefficients of different surfaces in steady state case for ventilated discs with materials FG25 AL, FG20 and FG15

Materials	FG25 AL	FG20	FG15
Surface	$h_{average} = [W\ m^{-2}\ k^{-1}]$		
SC1	54.1624	53.9260	53.8749
SC2	84.6842	83.7842	83.6516
SC3	44.4171	44.3485	44.3295
SF1 and 2	135.4039	135.0584	135.0007
SF3	97.1710	95.0479	94.8256
SPV1	170.6472	171.4507	171.5696
SPV2	134.0815	134.3285	134.3615
SPV3	191.2441	191.9436	192.0391
SPV4	175.1667	176.13340	176.2763
ST1	113.6098	114.3962	114.3916
ST2	35.0993	34.4723	34.3473
ST3	68.3316	66.3316	66.0317
ST4	75.0945	72.1235	71.6642
SV1	135.5299	131.1183	131.2075
SV2	119.2572	118.4648	118.2040
SV3	46.7023	44.8195	44.5264
SV4	111.5769	108.5044	108.1817

The velocity contour is plotted in Fig. 26. The velocity distribution on the vane surface channels (channels) in the ventilated brake disc of the vehicle is well marked using CFX Pre software whose speed is low just at the exit of the disc at vanes.

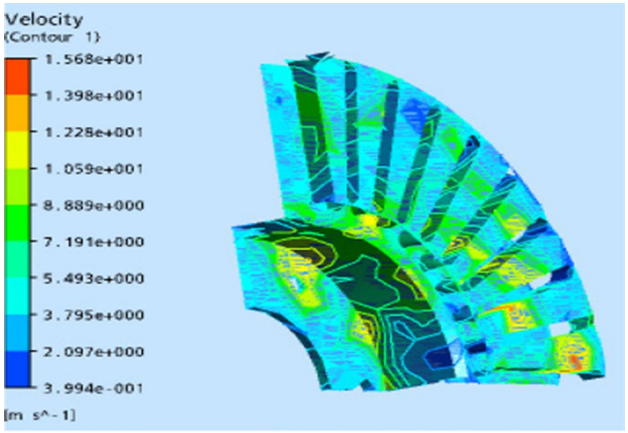

Fig. 26 Velocity contour of ventilated disc rotor

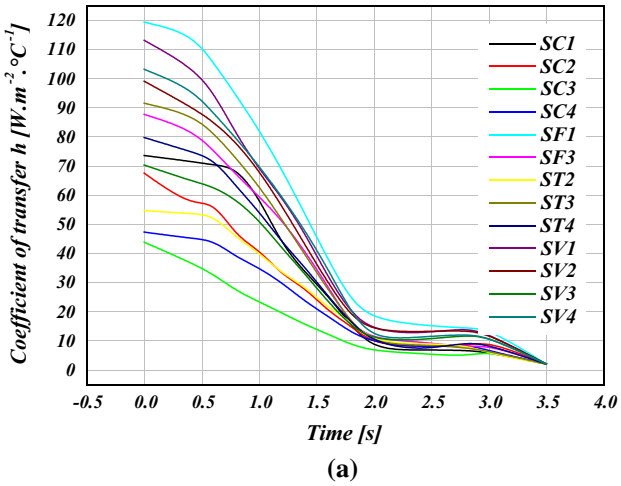

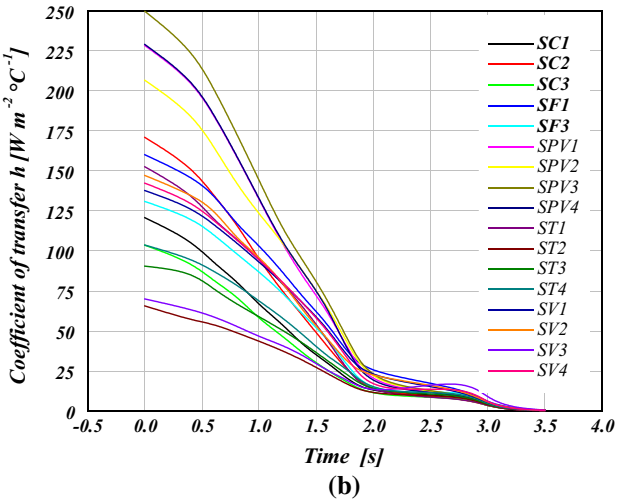

Fig. 27 Heat transfer coefficient *(h)* versus time at different disc surfaces at material FG15 in transient thermal case for **a** full disc faces, and **b** ventilated disc

8.2 Transient cases

8.2.1 Evaluation of the heat exchange coefficient (h)

Heat transfer coefficient of the wall (h) is a physical quantity which is related to the geometric design of the brake disc, the velocity of the air circulation, as well as other parameters attached to the braking process. Indeed, when vehicle moves in motion, the heat exchange coefficient (h) in the company of air changes with the speed of the disc, it depends on the form of braking medium. In transient situation, this convective heat exchange coefficient (h) is variable as function of time on each disc surface [40]. This one, practically, has nothing to do with the material, but, it depends on the surface geometry as well as the conditions of law of the convective regime.

Figure 27a, b show the evolution of the heat transfer coefficient (h) at each surface of the full and ventilated disc, as function of time. We used these two graphs later to predict the three-dimensional distribution of the two brake discs. It can be said that the values of the convective heat exchange coefficient (h) vary according to the geometric design of the disc, whether it is full or ventilated and, it is quite rational that the aeration generates the decrease of the maximum temperatures at the walls. The variations of the wall heat transfer coefficient as function of time for insulated surfaces SV1 and SPV2 respectively belong to the full and ventilated brake disc for material FG15 are clearly shown in Fig. 28a, b.

9 Results and discussion of FEM analysis

9.1 Model validation against experimental data

The analysis in this work is compared to available literatures to ensure the reliability of the results. Figure 29 shows the time variation of the observed disc temperature against the values from [39]. Figure 29 shows that the temperature results from both the thermocouple and the finite element software ANSYS 11.0 of the ventilated disc brake made of material FG15 are very similar. It is believed that the response of the thermocouple is a little slower in cooling than heating due to residual heat in its rubbing components. But the variation is so small as shown in the figure, such that it was decided that the level of accuracy of rubbing type thermocouples used in the experimental stages of this research is acceptable. It can also be concluded that the transient thermal simulation of the ventilated disc, performed by the finite element method, gives us good correlation with the thermocouple measurements.

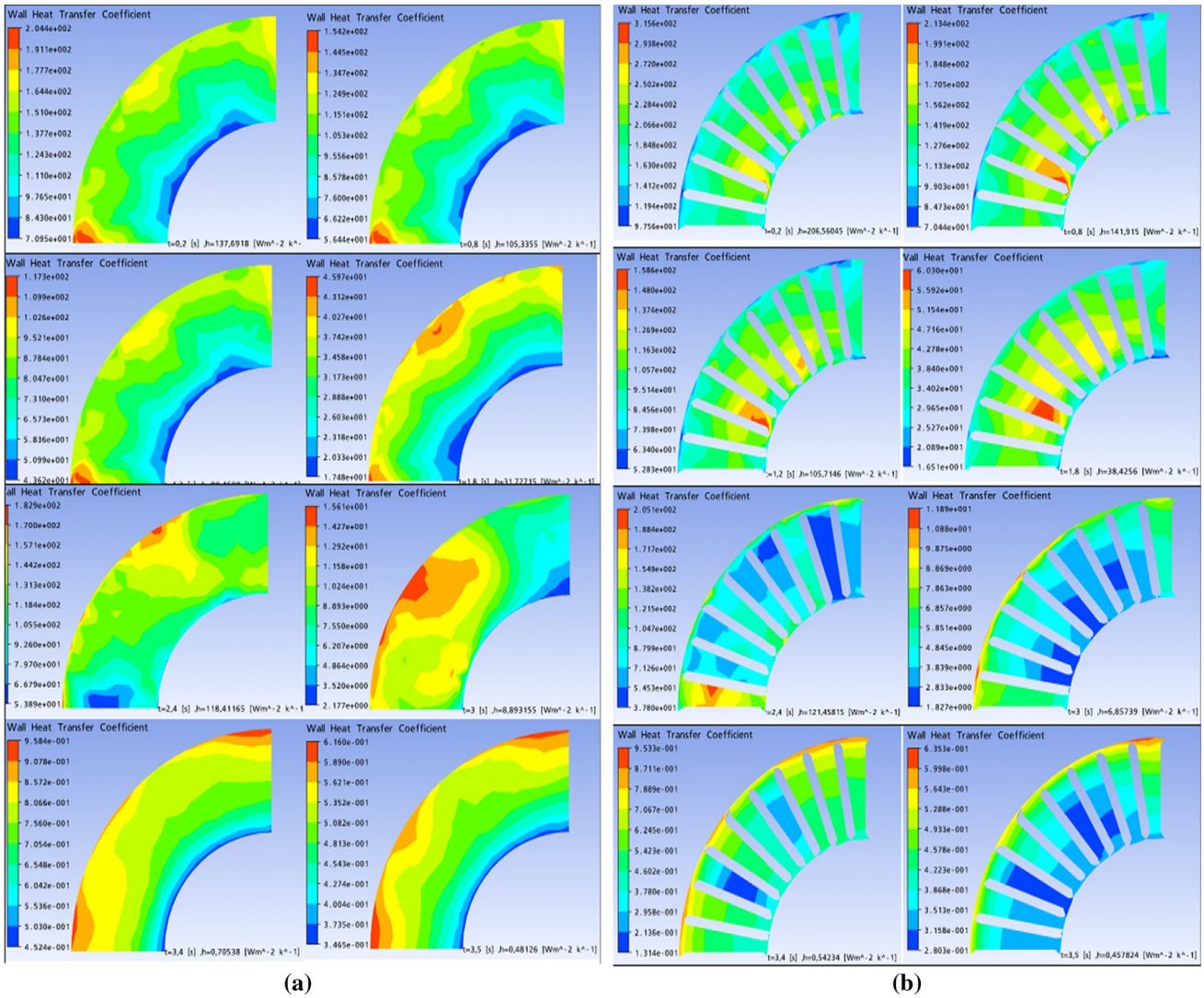

Fig. 28 Variation of the heat transfer coefficients (h) in specific time sequence of the discs with FG15 material. **a** Surface SV1 of the ventilated disc and **b** Surface SV2 of the full disc

9.2 Results of the disc temperature

In order to perform multi-step analysis, and to simulate the thermal behavior of full and ventilated disc brake, we used the ANSYS Workbench 11.0 software during the transient thermal analysis. The inner and outer faces of the brake disc are designed to generate symmetrical heat flow upon mutual sliding of the disc when it is rotated around the brake pads. During this cyclic mechanism, we distinguish the alternation of two thermal phenomena associated with convection; it is in this case, the heating and cooling of the brake disc.

The transient thermal analysis of the two discs, full and ventilated brake discs were performed using finite element (FE) software. The calculation does not last very long, which is positive point. The results of the temperature distribution (3D) for the three materials namely; the gray cast iron FG25AL, FG20, and FG15 are provided in Fig. 30. It should be understood that the material having lower thermal conductivity thus generates important thermal gradients and consequently increase in the surface temperature of the brake disc. To make the choice of material and to know if it is profitable, we tested the one that cools better, it is necessary to remember that one wants to have material which does not preserve the heat. From the results provided by this simulation, it can be seen that the ventilated discs made of the materials FG20 and FG25AL, respectively, having temperatures reaching 351.5 and 380.2 °C, which in turn, are greater than that of the ventilated disc of material FG15 having a maximum temperature of 345.4 °C as indicated in Fig. 31. It can thus be concluded that the most suitable material in this case for the brake discs is the gray cast iron FG15 which presents the better thermal performance.

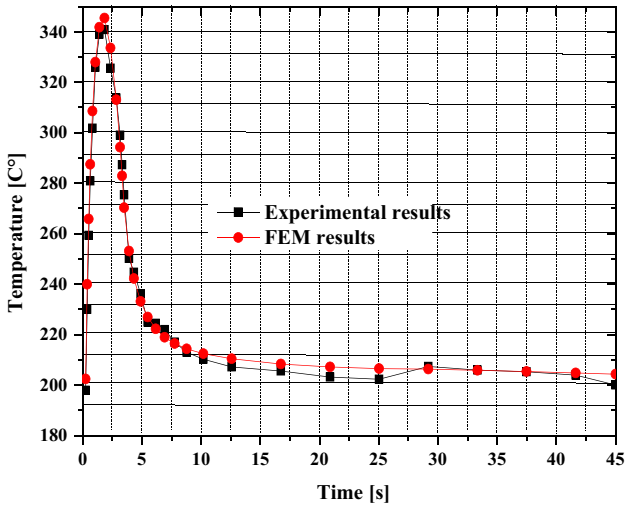

Fig. 29 Validation of the FEM model against experiments by Stephens [39]

Figure 32 shows the temperature of the brake disc at time t = 1.8 s reaching maximum value of 401.5 °C, and after that, it decreases exponentially at 4.9 s until it reaches braking cycle termination at instant, t = 45 s. The forced convection step is well designated in the temporary interval between the instant 0 s and 3.5 s, as shown in Fig. 32. On the other hand, the natural or free convection is quite marked after the duration of the forced convection arriving at the end of braking time, which is the total time of the simulation (t = 45 s). It can be seen from the graphs that the temperature of the full brake disc exceeds that of the ventilated disc with difference of 60 °C. Finally, we can draw the conclusion that the ventilated brake disc allows us to provide better cooling therefore, better endurance and gives us ability to dissipate more heat for braking efficiency.

10 Coupled thermo-mechanical analysis

Braking is a complex problem due to the coupling between thermal, thermomechanical, tribology and dynamics of the scale of the structure at the contact scale. Under the effect of the heat generated by the braking, the disc deforms, causing in turn, a location of the contact and therefore a concentration of the heat flow on the disc. The thermomechanical deformations of the disc are therefore directly related to the surface thermal gradients. The purpose of analysis is to present modelling of the model (disc-brake pads) in a thermomechanical coupling. The procedure for coupled field analysis depends on which fields are being coupled, but two distinct methods can be identified: direct and sequential (load transfer). The sequential method which it is about here, involves two or more sequential analyses, each belonging to a different field. You couple the

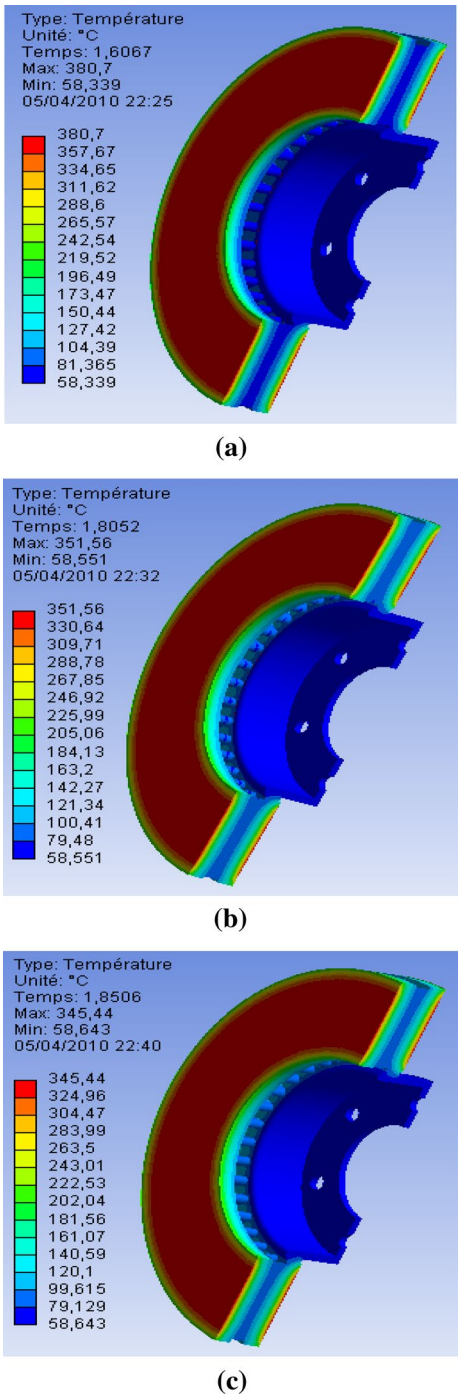

Fig. 30 Temperature plot of ventilated discs for three materials gray cast iron **a** FG25 AL, **b** FG20, and **c** FG15

two fields by applying results from the first analysis as loads for the second analysis. The thermomechanical calculation is carried out in two stages with weak coupling. Firstly, a thermal calculation simulates the thermal flux imposed on the surface of the disc during stopping braking leading to thermal expansion. In a second step, a mechanical calculation makes it possible to evaluate the stresses induced by the thermal expansion.

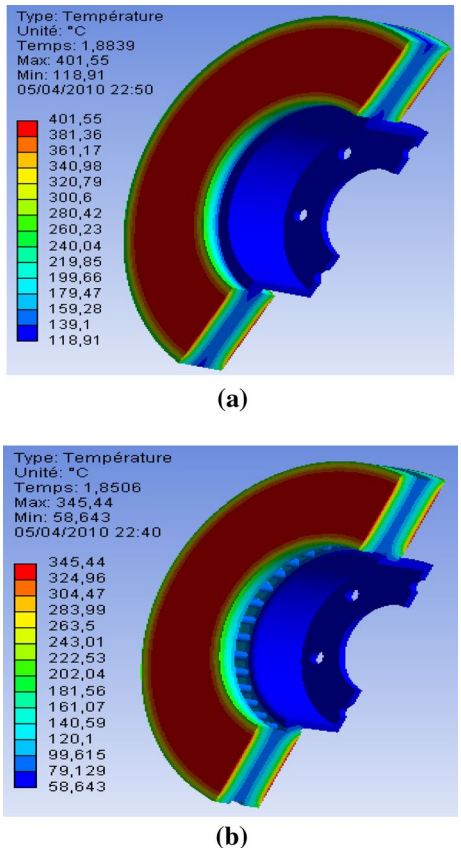

Fig. 31 Temperature plot on disc brake of the same material (FG15). **a** Full disc, **b** Ventilated disc

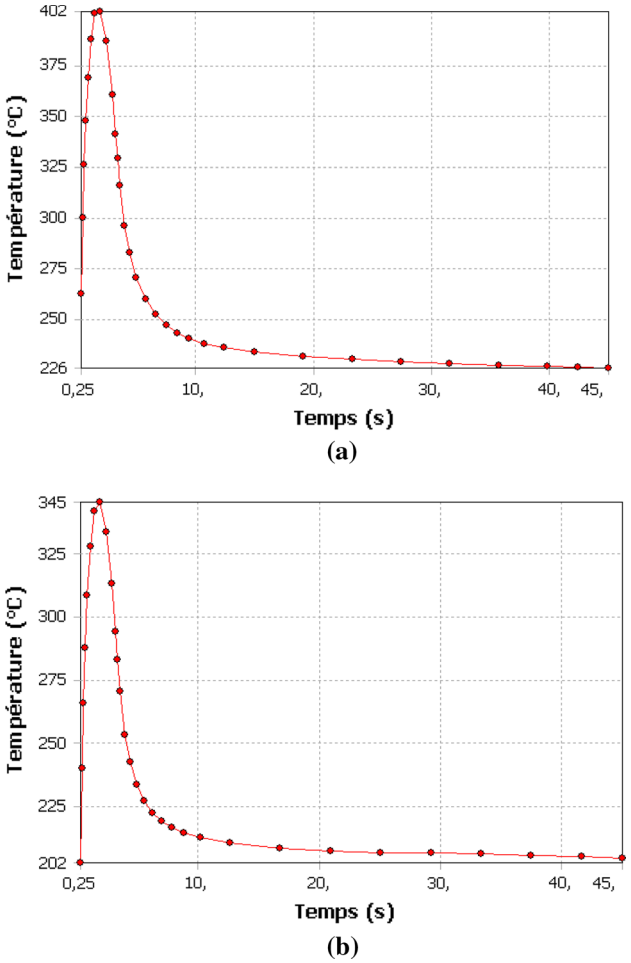

Fig. 32 Disc temperature versus time for **a** full disc and **b** ventilated disc, for material gray cast iron FG15

Thus, the mechanical calculation is influenced by the thermal calculation but the reciprocal is false (Fig. 33).

10.1 Calculation of hydraulic pressure

In order to proceed with the preliminary mechanical calculation, we determined the constant value of the hydraulic pressure exerted by the piston on the inner brake pad. For this, we assumed that the rate of 60% of the braking forces is maintained both front brake discs, giving a percentage of 30% for each rotor [41]. So, using the data in Table 5, we can thus calculate the typical force of a single rotor as follows (see Annex A for more detail):

$$F_{disc} = \frac{(30\%)\,\frac{1}{2}\,m v_0^2}{2\,\frac{R_{rotor}}{R_{tire}}\left(v_0\,t_{stop} - \frac{1}{2}\left\{\frac{v_0}{t_{stop}}\right\}t_{stop}^2\right)} = 1047.36\,[N] \quad (14)$$

The angular velocity of the rotor can be evaluated as follows

$$\omega = \frac{v_0}{R_{tire}} = 157.89\ \text{rad/s} \quad (15)$$

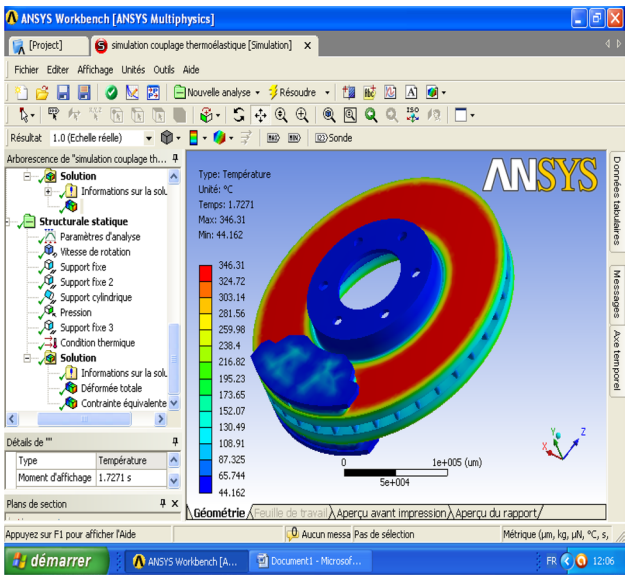

Fig. 33 Thermomechanical coupling analysis in ANSYS Multiphysics

Table 5 Vehicle data

Item	Value
Vehicle mass—m (kg)	1385
The initial velocity—v_0 (m/s)	60
Duration of braking application (s)—t_{stop}	45
The effective radius of the disc—(mm)	100.5
The radius of the wheel—(mm)	380
Friction coefficient disc/pad μ (/)	0.2
Pad surface A_c (mm^2)	5246.3

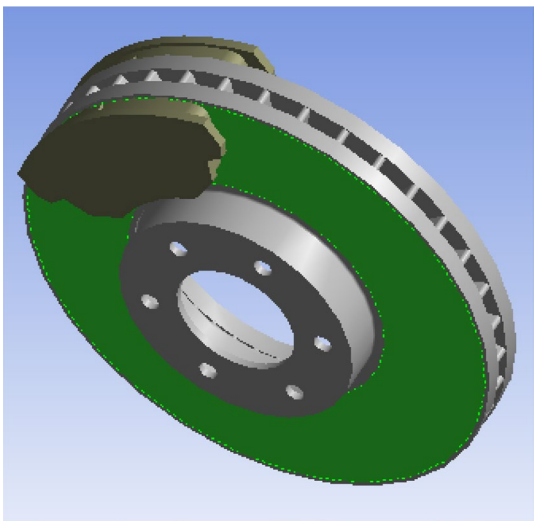

Fig. 34 Contact surface of the disc

We used ANSYS Workbench software to determine the entire area of the disc friction track swept by the brake pads during rotation while selecting on this contact surface that is equal to 35,797 mm^2, as it is shown in green color on Fig. 34 below.

Using the above calculations, the value of the hydraulic pressure P is obtained from the following form [42]

$$P = \frac{F_{disc}}{A_c \mu} = 1 \text{ [MPa]} \tag{16}$$

where μ, is the friction coefficient, A_c is the surface of the brake pad in contact with the brake disc, which is obtained directly from simple selection in ANSYS Workbench. In our case, it is indicated in green in Fig. 35 and equal to at 5246.3 mm^2.

10.2 Elastic problem

The mechanical stress is linked to the effort by a constitutive equation following:

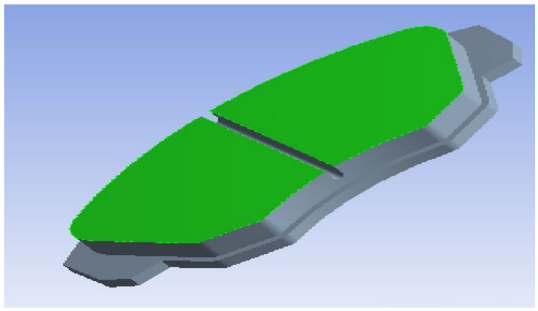

Fig. 35 Contact surface of the pad

$$\{\sigma\} = [D]\,\{\varepsilon^{me}\} \tag{17}$$

where [D] is the material property matrixThe total stress, sum of the mechanical and thermal stresses, is given by:

$$\{\varepsilon\} = \{\varepsilon^{me}\} + \left\{\varepsilon^{th}\right\} \tag{18}$$

where the upper indices (me) and (th) denote mechanical and thermal stresses, respectively,Equation (17) becomes:

$$\{\sigma\} = [D]\left\{\{\varepsilon\} - \left\{\varepsilon^{th}\right\}\right\} \tag{19}$$

where $\{\sigma\} = \left\{\sigma_r \sigma_\theta \sigma_z \sigma_{r\theta}\, \sigma_{\theta z} \sigma_{zr}\right\}$, $\{\varepsilon\} = \left\{\varepsilon_r \varepsilon_\theta \varepsilon_z \varepsilon_{r\theta}\, \varepsilon_{\theta z} \varepsilon_{zr}\right\}$.

For isotropic material, temperature change results in body expansion or shrinkage but no deformation. In other words, the temperature change affects the normal stresses without shear stresses.

The thermal stress vector is expressed as follows:

$$\left\{\varepsilon^{th}\right\} = \{\alpha \Delta T\ \alpha \Delta T\ \alpha \Delta T\ 0\ \ 0\ \ 0\}$$

which α, is the coefficient of thermal expansion and ΔT indicates the temperature difference. Total stress is expressed in terms of nodal displacements as

$$\{\varepsilon\} = [B]\,\{d\} \tag{20}$$

where [B] is the kinematic matrix.

Substitute (20) in (19), we will have:

$$\{\sigma\} = [D]\,[B]\,\{d\} - [D]\left\{\varepsilon^{th}\right\} \tag{21}$$

The weighted residual method is applied to Eq. (21) and the results are found in the following equation

$$[K]\,\{d\} = \left\{F^{th}\right\} + \{F^{me}\} \tag{22}$$

where the elemental stiffness matrix for elasticity is given in the form:

$$[K^e] = \int_{\Omega^e} [B]^T [D]\,[B]\, d\,\Omega \tag{23}$$

$\{F^{th}\}$ and $\{F^{me}\}$ are the thermal and mechanical force vectors that are denoted as follows:

$$\{F^{th}\} = \int_{\Omega} N^T N\, d\,\Omega$$

$$\{F^{me}\} = \int_{S} N^T N\, d\, S$$

The elastic problem is solved by employing the constitutive equation. During numerical modeling, special attention is required to satisfy the continuity of normal displacements on the contact surface and the overlap conditions [43].

The following conditions of movement and effort are imposed on each pair of nodes on the interface

$$W_i = W_j \text{ when } P > 0;\ W_i \neq W_j \text{ everywhere} \tag{24}$$

$$\sigma_{zj} = -\sigma_{zj} \text{ when } P > 0;\ \sigma_{zj} \neq \sigma_{zj} \text{ everywhere} \tag{25}$$

The following conditions of temperature and heat flux constraints are imposed on each pair of nodes on the interface

$$T_i = T_j \text{ when } P > 0;\ T_i \neq T_j \text{ everywhere} \tag{26}$$

$$q^* = \mu P \omega r \text{ when } P > 0; \quad q^* = 0 \text{ everywhere} \tag{27}$$

10.3 FE model and boundary conditions

The boundary conditions applied to the model result from the assumptions and model choices presented above. Figure 36a, b show the boundary conditions imposed on FE model, consisting of brake disc and two brake pads in dry contact in the case of pressure exerted on one side of the pad and that of double pressure on both sides of the pad.

As we have done thermal analysis, the conditions to be taken into account are those which will influence the thermal phenomena such as the ambient temperature which is the initial temperature of disc 20 °C, the thermal flow and that of convection imposed on all the surfaces of the brake disc while for the two brake pads [44], convection heat exchange coefficient (h) of value 5 W/m^2 °C is applied on their outer surfaces on both sides (Fig. 37).

For structural boundary conditions, we know that the brake disc is fixed to the mounting holes thus requiring fixed support on these holes taking into account its rotational speed [22] ω = 157.89 rad/s. The internal disc

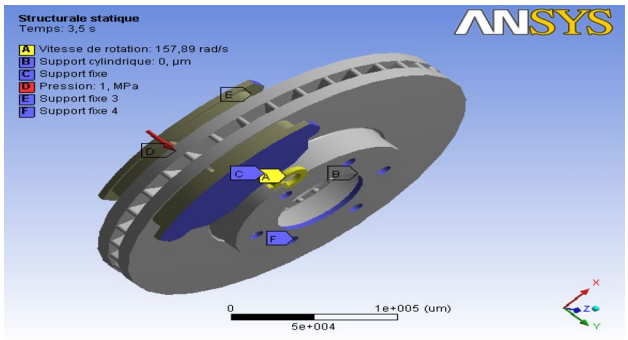

(a)

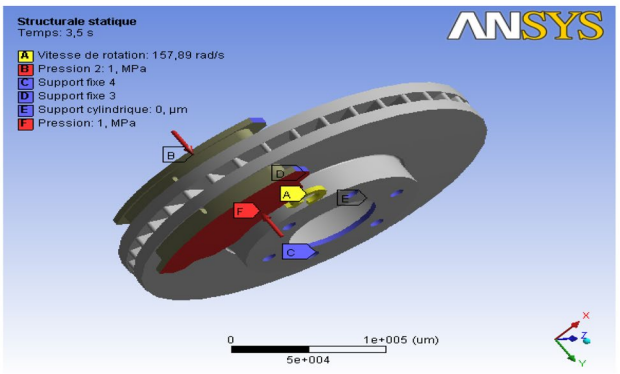

(b)

Fig. 36 Loading conditions for disc brake assembly. **a** One piston, **b** Two pistons

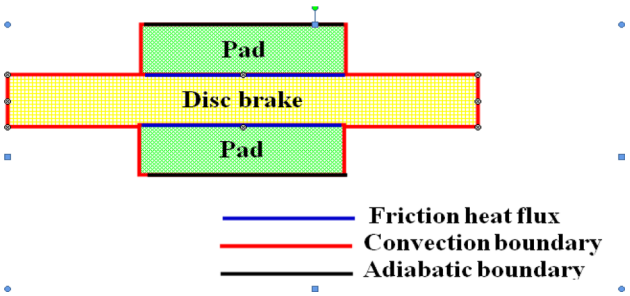

Fig. 37 Thermal boundary condition applied to the model

diameter is sustained at fixed support for both radial directions while the tangential direction is left free in this simulation.

The structural boundary conditions applied to pads are also introduced. We imposed pressure of 1 MPa on the piston pad while maintaining fixed support on the finger pad while on the contact surface; the pad is assembled on its edges at the perpendicular plane. The friction between the two parts (disc-brake pad) is defined by a coefficient equal to 0.2.

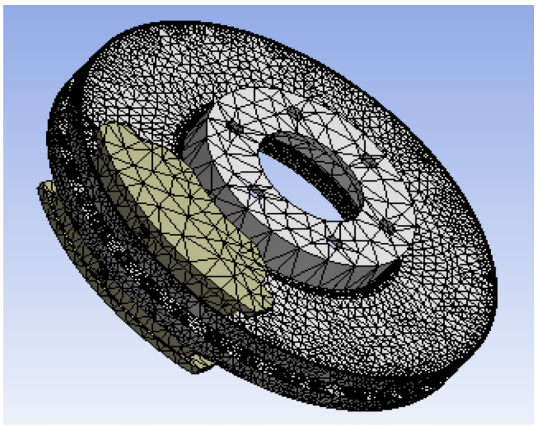

Fig. 38 Meshed model of disc brake assembly

10.4 Geometry and mesh

Three-dimensional mesh of ventilated disc was generated using the ANSYS software (Fig. 38). Parts were meshed with element types of 10 Node Quadratic Tetrahedron (Solid 187). It is elementary solid respecting the periodicity of the fasteners of the bowl and internal cooling fins, representing entire disc. The brake disc is divided into two volumes to allow refinement of the mesh of the friction tracks. The first volume consists of two friction tracks. The mesh is three-dimensional (3D) tetrahedral type with 10 nodes, regular on the friction tracks and more fine as one approaching the friction surfaces. The second volume consists of the remaining disc with the bowl and the internal cooling fins. The total number of nodes is 185901 while the total number of elements is 113367. A frictional contact pair was defined between disc-pad interfaces. Element types used were Quadratic triangular Contact (Conta 174) and Quadratic triangular Target (Targe 170).

10.5 Thermal distortion

The pressure distribution and the actual contact area vary as long as there is thermal deformation during the braking process. The mechanical and thermal deformations overlap with each other as whole from which the deformation of the disc has become very large in its circumference and decreases gently in its radial direction, of which this is well exposed in its lateral section because of the presence of thermal loading. Indeed, frictional heating causes non-uniform pressure distribution between the brake pads and the brake disc which causes its thermal deformation. In other words, the deformation of the brake disc area is mainly due to the thermal expansion of the brake disc material.

Figure 39 shows the maps of the total deformation of the whole model (disc-brake pads) evaluated at times t = 1.7271 s, 3.5 s, 30 s and 45 s. According to this figure, the maximum total deformation recorded at time t = 3.5 s is of the order of 284.55 µm, where it coincides with the braking moment. It is obvious that strong distribution amplifies with time as well on the friction tracks of the disc and its outer ring that its fins of cooling. Indeed, at the beginning of the braking, relatively homogeneous, relatively homogeneous, hotspots appear on the friction tracks of the disc. During braking, this hot strip with hot spots gradually migrates to the inner radius. Hot spots intensify to form stationary macroscopic hot spots at the inner radius. At the end of the braking, the intensity decreases and the surface gradients homogenize. The migration of the locations is explained by the difference in expansion between the track of the disc and its rear face, leading to "umbrella" deformed disc during warm-up. Deformation of the structure therefore, has preponderant role in the migration of thermal locations.

10.6 Von Mises stress distribution

The model provides access to Von Mises stress distribution mapping at the start of braking (Fig. 40) and after cooling the sector to ambient temperature. The distribution is well noted here in order ranging from 0 to 495.56 MPa. The great value recorded during this modeling in thermomechanical coupling is very significant when compared to mechanical dry contact analysis under the same braking conditions. According to the established conclusion, the Von Mises stresses are maximums in the outer band at the level of the brake disc bowl at the instant 3.5 s, corresponding to the moment when the thermal gradient in the track thickness is the most important. Indeed, the brake disc is fixed to the hub by bolts in order to prevent its movement and as soon as it starts to rotate, torsion and shear stresses have just been produced at the level of its bowl which generates automatically stress concentrations around its fixing holes. The disc bowl thus risks mechanical rupture under repetitions of these undesirable effects during the braking process.

The general evolution of the stresses in the disc during the braking-cooling cycle is in agreement with the phenomena described in the previous literature searches.

10.7 Contact pressure distribution

The braking operations are characterized by the sliding speed, the apparent contact pressure, the braking time, the energy dissipated by the brake and the initial braking power. The heat generated on contact and the wave deformation of the disc caused by the differences in thermal expansion lead to the migration of the contact in the form of hot band on the circumference of the disc. Within this hot band, contact pressures and the dissipated energy are very high. The contact is said to be closed in the hot band zone and otherwise open.

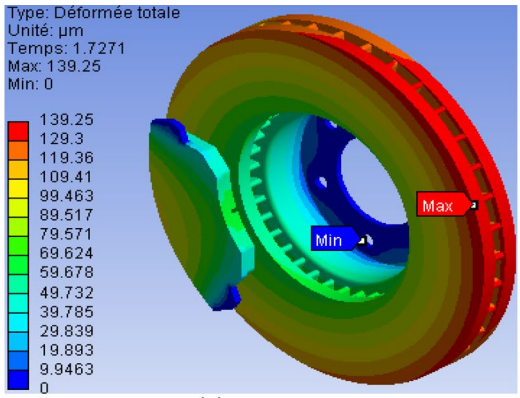

(a) t=1.7271 s

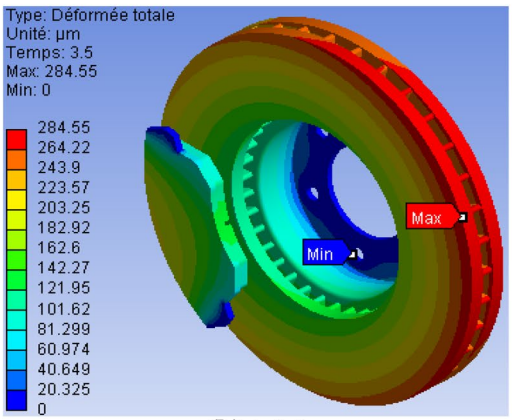

(b) t=3.5 s

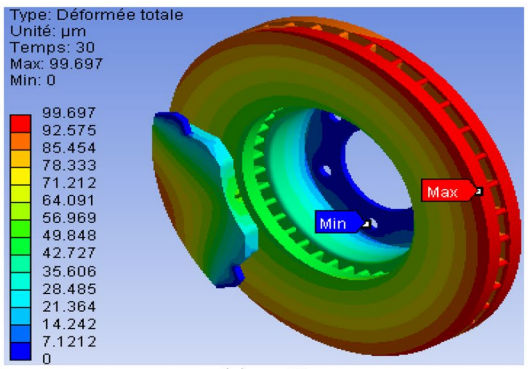

(c) t=30 s

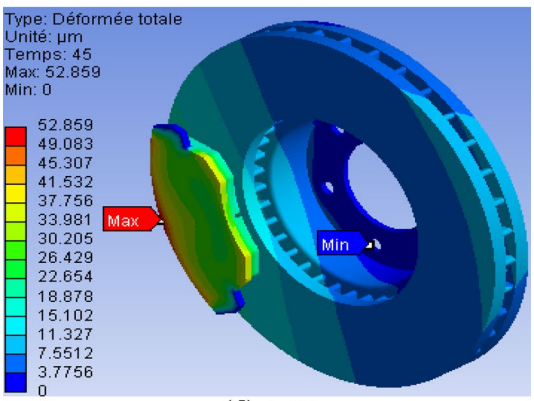

(d) t=45 s

Fig. 39 Total deformation of disc-pad model

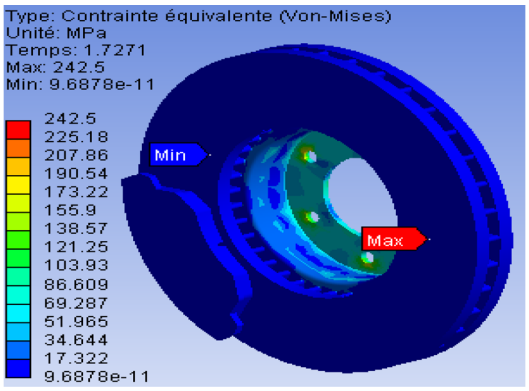

(a) t=1.7271 s

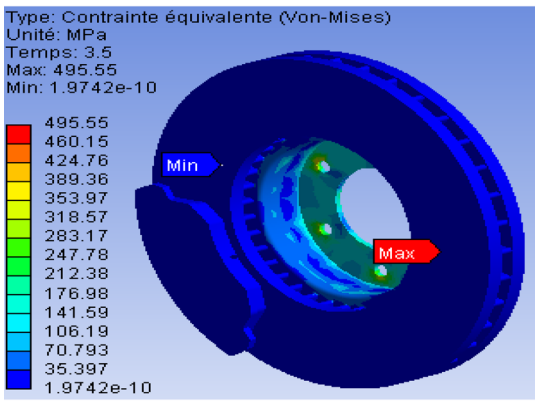

(b) t=3.5 s

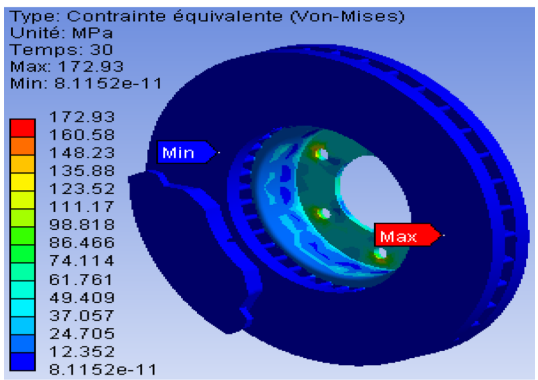

(c) t=30 s

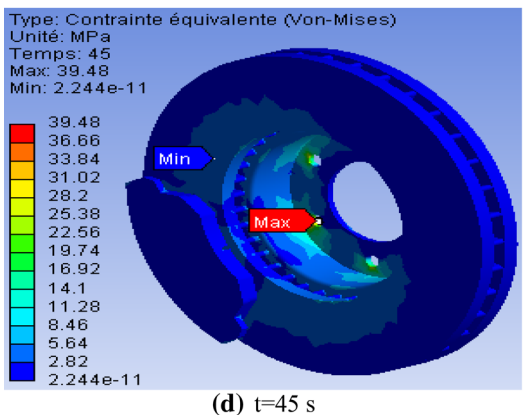

(d) t=45 s

Fig. 40 Von Mises equivalent stress obtained step by step

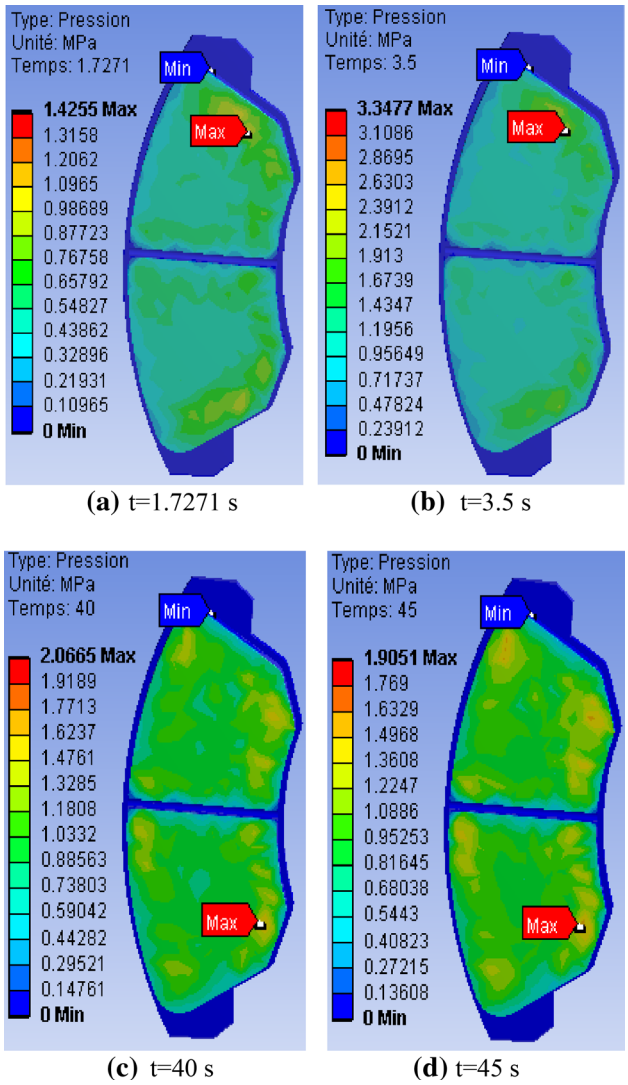

Fig. 41 Contact pressure distribution in the inner pad

After the passage of the hot band, in the open hot zone, third body debris is observed on the surface of the disc. These powders recirculate in contact with the rotation of the disc.

Figure 41 shows mapping of the contact pressure at the friction interface between the inner brake pad and brake disc with various simulation times. In these, the maximum contact pressures evaluated are of the order of 3.3477 MPa at the instant when the rotational speed is zero t = 3.5 s. It can also be seen that this maximum value is in the leading edges of the pads towards the trailing edge by friction. Moreover, the distribution of the contact pressure is quite symmetrical with respect to the groove of the brake pads. In the thermomechanical coupling that we carried out here, it is clear that the contact pressures are not negligible and can reach locally very high values, of the order of GPa. The plastic flow observed in the sliding direction attests well to the severity of the friction forces, so very high contact pressure.

10.8 Von Mises stress at inner pad

In order to study the influence of the groove of the brake pads as well as loading modes applied to the pistons (single-pressure and double-pressure). We solve the model and ask for the equivalent Von Mises stress of three different designs. Brake pads in this case, brake pad with center groove subject to single double piston. We obtain the following visuals that are grouped in Figs. 42a–g. It can be seen that almost all the contact pads of the brake pads are dressed in dark blue color meaning low stresses at the beginning of the braking moment (t = 1.7 s). Nevertheless, from the moment of the end of braking t = 45 s, the scale of Von Mises stress becomes more important whose vision of the colors becomes practically blue ocean whose distribution is well noticed on the three conceptions. It can be concluded that the existence of the groove in the brake pad and the presence of a mechanical double piston loading have positive influence on the stress distribution on the brake pad.

11 Conclusion

In the transport sector, braking is major problem. It is question of obtaining from this systematic safety equipment reliability with acceptable cost, whereas the phenomena which are attached to it are complex.

In general, from a thermal point of view, the braking system is considered to be composed of only three elements: the disc in motion at variable speed, on which are rubbed the two pads which are subjected to pressure evolving over time. The phenomenon of induced friction generates a dissipation of thermal power at the interface and causes sharp increase in temperature that may deteriorate the equipment. The temperature level reached is directly related to the way in which the heat is transferred into its immediate environment, that is to say the disc and the two pads.

In this paper, a thermomechanical analysis of disc brake rotor with gray cast iron material properties has been performed. A model qualification method has been presented here as a tool for mechanical model assessment in interactive simulations.

First, we presented complex modeling of convection-driven brake discs in order to predict the heat transfer coefficients (h) during the aerodynamic conditions of the braking stage by using the ANSYS CFX software. Heat transfer coefficients (HTC) have been used in calculating the heat transfer, typically by convection or phase transition between a fluid and a solid. The heat transfer coefficients (HTC) of the brake disc's ventilation are estimated by means of a CFD approach. In this analysis, the speed of the vehicle was used to determine the heat generated by the braking taking into account all the parameters involved

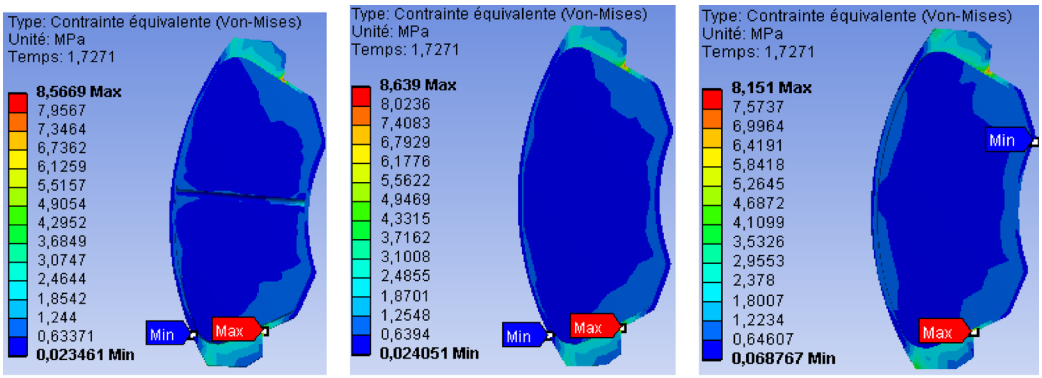

(a) at time t= 1.7s

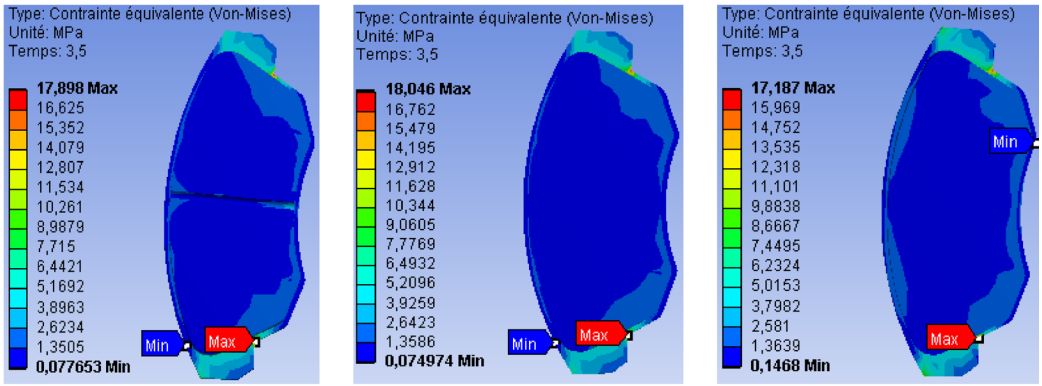

(b) at time t= 3.5s

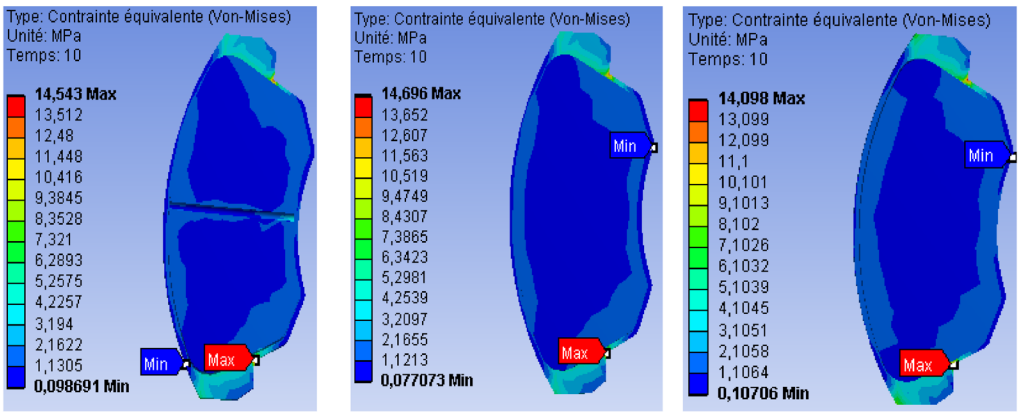

(c) at time t= 10s

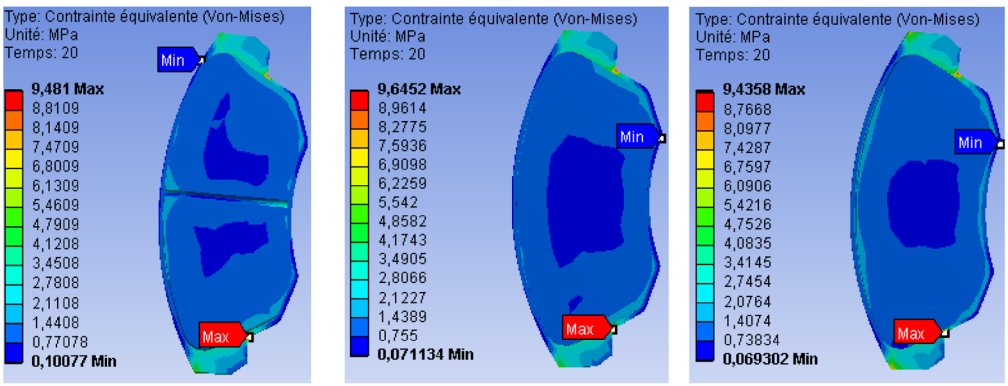

(d) at time t= 20s

Fig. 42 Distribution of Von Mises stress at different braking time: Single piston with pad center-groove (left), Single piston without groove (center) and Double piston without pad groove (right)

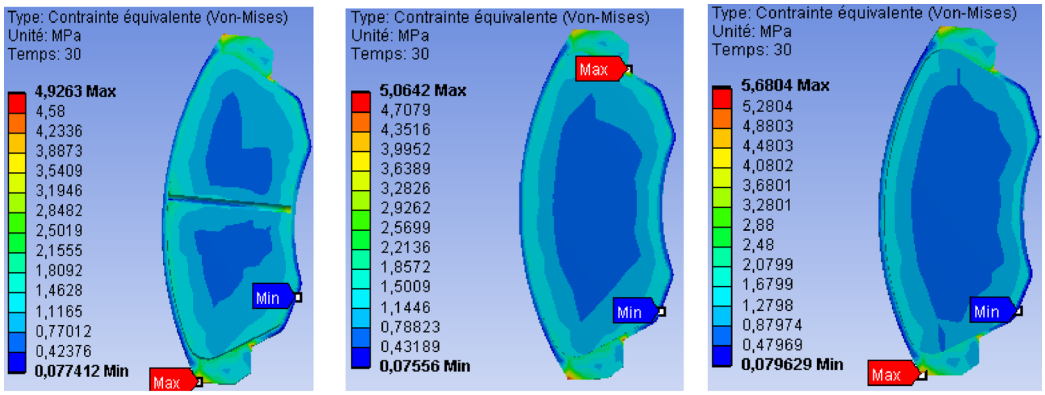

(e) at time t= 30s

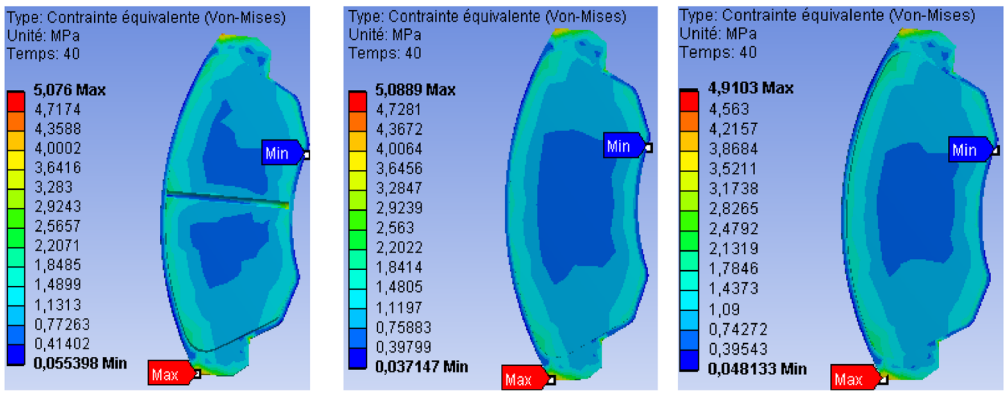

(f) at time t= 40s

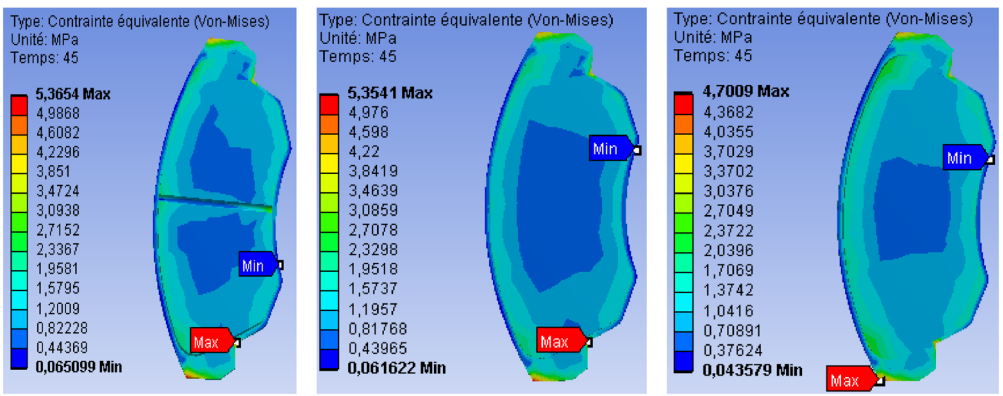

(g) at time t= 45s

Fig. 42 (continued)

which affect the net heat generation and dissipation from the brake disc. Thus we have determined the temperature rise in the brake disc and have found a working temperature range of the brake. This technique of predicting the operating temperature of the brakes can be used for several purposes. In order to withstand both thermal and mechanical loading and knowing in advance, the operating temperature of the brakes, we can select the material used to manufacture the brake components, such as brake disc, caliper, etc.

This research was conducted to study the relationship of the brake disc geometry towards the best braking performance in term of heat dissipation in the environment. From the results, it shows that ventilated disc brake has faster heat dissipation rate to surrounding compare to full disc brake. Thus, the ventilated disc brake is having better braking performance than full disc brake in terms of heat dissipation rate. The results were also validated using the temperature–time profile from both the simulated and experimental results, in which the two results were found to be in good

agreement. The literatures for ventilated brake disc with gray cast iron FG15 also gives good agreement with results from literatures.

In this research, we simulated the disc-pad model by employing a coupled thermomechanical approach. From the prediction results, the following conclusions can be derived:

- At the level of the outer radius and the outer ring of the brake disc, large deformation occurs seriously.
- In pad without groove and that subjected to double pressure, the stresses are significantly intensified during braking.
- The temperature has significant effect on the thermomechanical behavior of the braking system. Thus, with thermal effect, contact pressure distribution of pad and the global deformation of the brake disc are quite important.

However, it seems to us that several thermomechanical aspect that need to be considered in more detail in the topic of automotive braking system, particularly essentially for more quantitative assessment of damage in materials life approach.

Design engineers using the interactive design approach to obtain the optimal design of system. Additional thermomechanical predictions could be taken into account to better interpret the effect of thermal stress migration on fatigue life of brake discs.

Compliance with ethical standards

Conflicts of interest The authors declare that there is no conflict of interest.

Appendix A

A.1. Analysis of disc rotor force

A free body diagram of a front wheel-rotor system, Fig. 43, is used to drive the equation of equilibrium. Since large amount of the braking load is born by the front brakes, that amount of kinetic energy and potential energy into a single disc is given by

$$E_{dissipated} = \frac{1}{2} k m v_0^2 + S_b m g \sin \alpha \tag{A.1}$$

But $S_b = \frac{v_0^2}{2a}$

$$E_{dissipated} = \frac{1}{2} k m v_0^2 + \frac{v_0^2}{2a} m g \sin \alpha \tag{A.2}$$

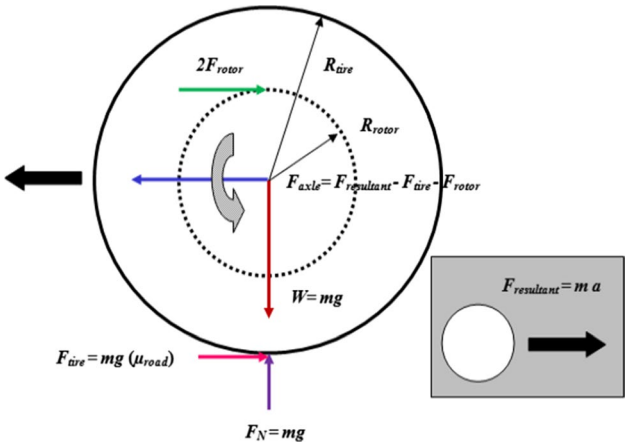

Fig. 43 Free body diagram of a front wheel-rotor system

The power dissipated by each rotor face is equal to the heat flux into the rotor face.

$$E_{dissipated} = \int P_{dissipated}\, t\, dt = \int (2 F_{rotor})\, v_{rotor}(t)\, dt \tag{A.3}$$

$$\frac{1}{2} k m v_0^2 + \frac{v_0^2}{2a} m g \sin \alpha = K E_{dissipated} =$$

$$\int P_{dissipated}\, t\, dt = 2 \int F_{rotor}\, v_{rotor}(t)\, dt \tag{A.4}$$

But from kinematic relationships.

$$v_{vehicle}(t) = v_0 - a t$$

$$a = \frac{v_0}{t_{stop}}$$

$$\frac{v_{vehicle}(t)}{R_{tire}} = \omega(t) = \frac{v_{rotor}(t)}{R_{rotor}}$$

$$v_{rotor}(t) = \frac{R_{rotor}}{R_{tire}} \left(v_0 - \left\{ \frac{v_0}{t_{stop}} \right\} t \right)$$

F_{rotor} is constant with respect to time, and v_{rotor} varies only linearly with time so the energy balance equation becomes:

$$\frac{1}{2} k m v_0^2 + \frac{v_0^2}{2a} m g \sin \alpha = 2 F_{rotor} \int_0^{t_{stop}} v_{rotor}(t)\, dt$$

$$= 2 F_{rotor} \frac{R_{rotor}}{R_{tire}} \left(v_0 t_{stop} - \frac{1}{2} \left\{ \frac{v_0}{t_{stop}} \right\} t_{stop}^2 \right) \tag{A.5}$$

$$F_{rotor} = \frac{\frac{1}{2} k m v_0^2 + \frac{v_0^2}{2a} m g \sin \alpha}{2 \frac{R_{rotor}}{R_{tire}} \left(v_0 t_{stop} - \frac{1}{2} \left\{ \frac{v_0}{t_{stop}} \right\} t_{stop}^2 \right)} \quad \text{(A.6)}$$

When braking on a straight/flat track ($\alpha = 0$), k is estimated to be about 0.30. Therefore, equation (A.6) should be modified to be:

$$F_{disc} = \frac{(30\%) \frac{1}{2} m v_0^2}{2 \frac{R_{rotor}}{R_{tire}} \left(v_0 t_{stop} - \frac{1}{2} \left\{ \frac{v_0}{t_{stop}} \right\} t_{stop}^2 \right)} \quad \text{(A.7)}$$

References

1. Abdullah, O.I., Schlattmann, J., Majeed, M.H., Sabri, L.A.: The distribution of frictional heat generated between the contacting surfaces of the friction clutch system. Int. J. Interact. Des. Manuf. **13**(2), 487–498 (2019)
2. Cagin, S., Fischer, X., Delacourt, E., Bourabaa, N., Morin, C., Coutelier, D., Carré, B., Loumé, S.: β-NTF reduction and fast kriging simulation of optimal engine configurations. Mech. Ind. **18**(5), 509 (2017)
3. Sébastian, P., Chenouard, R., Nadeau, J.P., Fischer, X.: The embodiment design constraint satisfaction problem of the BOOTSTRAP facing interval analysis and genetic algorithm based decision support tools. Int. J. Interact Des. Manuf. **1**(2), 99–106 (2007)
4. Ordaz-Hernandez, K., Fischer, X., Bennis, F.: A mathematical representation for mechanical model assessment: numerical model qualification method. Int. J. Ind. Manuf. Eng. **1**(1), 23–33 (2007)
5. Ryberg, A.B., Bäckryd, R.D., Nilsson, L.: A meta model-based multidisciplinary design optimization process for automotive structures. Eng. Comput. **31**(4), 711–728 (2015)
6. Fischer, X., Coutellier, D.: Research in Interactive Design, vol. 2. Springer, Berlin (2006)
7. Ordaz-Hernandez, K., Fischer, X., Bennis, F.: Validity domains of beams behavioral models: efficiency and reduction with artificial neural networks. Int. J. Comput. Intell. **4**(1), 80–87 (2008)
8. Ordaz-Hernandez, K., Fischer, X., Bennis, F.: Towards a modeling methodology for virtual prototyping in interactive design. In: Proceedings of Virtual Concept 2005
9. Botkin, M.E.: Structural optimization of automotive body components based on parametric solid modeling. Eng. Comput. **18**(2), 109–115 (2002)
10. Makrahy, M.M., Ghazaly, N.M., Abd El-Gwwad, K.A., Mahmoud, K.R., Abd-El-Tawwab, Ali M.: Optimization of a new wedge disc brake using taguchi approach. Int. J. Mod. Eng. Res. **3**(6), 3461–3465 (2013)
11. Singh, K.H., Kumar, A., Kumar, R.: Optimization of quality and performance of brake pads using Taguchi's approach. Int. J. Sci. Eng. Res. **5**(7), 632–639 (2014)
12. Bhat, R., Lee, K.S.: optimization of the brake parameter for a disc brake system to improve the heat dissipation using Taguchi method. Int. J. Mech. Eng. Technol. **8**(7), 44–52 (2017)
13. Botkin, M.E.: Modelling and optimal design of a carbon fibre reinforced composite automotive roof. Eng. Comput. **16**(1), 16–23 (2000)
14. Kothawade, S., Patankar, A., Kulkarni, R., Ingale, S.: Determination of heat transfer coefficient of brake rotor disc using CFD simulation. Int. J. Mech. Eng. Technol. (IJMET) **7**(3), 276–284 (2016)
15. Belhocine, A., Abdullah, O.I.: Numerical simulation of thermally developing turbulent flow through a cylindrical tube. Int. J. Interact. Des. Manuf. **13**(2), 633–644 (2019)
16. Fischer, X.: The interaction: a new way of designing. Res. Interact. Des. **2**, 1–15 (2006)
17. García, M., Duque, J., Pierre, B., Figueroa, P.: Computational steering of CFD simulations using a grid computing environment. Int. J. Interact. Des. Manuf. **9**(3), 235–245 (2015)
18. Cucinotta, F., Nigrelli, V., Sfravara, F.: Numerical prediction of ventilated planing flat plates for the design of Air Cavity Ships. Int. J. Interact. Des. Manuf. **1**, 1–12 (2017)
19. Tang, J., Bryant, D., Qi, H.: Coupled CFD and FE thermal mechanical simulation of disc brake. In: Proceedings of the Eurobrake Conference, Lille, France (2014)
20. Carfagni, M., Governi, L., Volpe, Y.: Comfort assessment of motorcycle saddles: a methodology based on virtual prototypes. Int. J. Interact. Des. Manuf. **1**, 155–167 (2007)
21. Adamowicz, A., Grześ, P.: Convective cooling of a disc brake during single braking. Acta Mechanica et Automatica **6**(2), 5–10 (2012)
22. Ishak, M.R., Abu Bakar, A.R., Belhocine, A., Taib, J.M., Wan Omar, W.Z.: Brake torque analysis of fully mechanical parking brake system: theoretical and experimental approach. Ingenieria Investigacion y Tecnologia **19**(1), 37–49 (2018)
23. Belhocine, A., Ghazaly, N.M.: Effects of young's modulus on disc brake squeal using finite element analysis. Int. J. Acoust. Vib. **31**(3), 292300 (2016)
24. Atkins, M.D., Kienhöfer, F.W., Kim, T.: Flow behavior in radial vane disk brake rotors at low rotational speeds. J. Fluids Eng. **141**(8), 1–13 (2019)
25. Zhang, W., Cheng, C., Du, X., Chen, X.: Experiment and simulation of milling temperature field on hardened steel die with sinusoidal surface. Int. J. Interact. Des. Manuf. **12**, 1–9 (2017)
26. Devanuri, J.K.: Numerical investigation of aerodynamic braking for a ground vehicle. J. Inst. Eng. (India) Ser. C **99**(3), 329–337 (2018)
27. Morel, A., Bignonnet, A., Germain, G., Morel, F.: Teaching durability in automotive applications using a reliability approach. Int. J. Interact. Des. Manuf. **4**, 281–287 (2010)
28. Dulcey, G.F., Fischer, X., Joyot, P.: An experiment-based method for parameter identification of a reduced multiscale parametric viscoelastic model of a laminated composite beam. Multisc. Multidiscip Model Exp Des **1**, 291–305 (2018)
29. Cagin, S., Bourabaa, N., Delacourt, E., Morin, C., Fischer, X., Coutellier, D., Carré, B., Loumé, S.: Scavenging process analysis in a 2-stroke engine by CFD approach for a parametric 0D model development. J. Appl. Fluid Mech. **9**(1), 69–80 (2016)
30. Cagin, S., Fischer, X., Delacourt, E., Bourabaa, N., Morin, C., Coutellier, D., Carré, B., Loumé, S.: A new reduced model of scavenging to optimize cylinder design. Simul. Trans. Soc. Model. Simul. Int. **92**(6), 507–520 (2016)
31. Palmer, E., Mishra, R., Fieldhouse, J.D.: An optimization study of a multiple row pin vented brake disc to promote brake cooling using computational fluid dynamics. Proc. Inst. Mech. Eng. Part D. J. Automob. Eng. **223**(7), 865–875 (2009)
32. Reimpel, J.: Braking technology. Vogel Verlag, Würzburg (1998)
33. Cruceanu, C.: Frâne pentru vehicle feroviare (Brakes for railway vehicles), Ed. Matrixrom, Bucureşti, (ISBN 978-973-755-200-6, 388) (2007)
34. Dittrich, H., Lang, R.: Finite-element analysis of the thermal loads acting on a passenger car brake disk. Automobiltechnische Zeitschrift **86**(6), 265–269 (1984)
35. Fukano, A., Matsui, H.: Development of Disc- Brake Design Method Using Computer Simulation of Heat Phenomena, SAE 860634 (1986)

36. Gotowicki, P.F., Nigrelli, V., Mariotti, G.V., Aleksendric, D., Duboka, C.: Numerical and experimental analysis of a pegs-wing ventilated disk brake rotor with pads and cylinders. In: 10th EAEC Eur. Automot. Cong.–Paper EAEC05YUAS04–P5 (2005)
37. Khalid, M.K., Mansor, M.R., Abdul Kudus, S.I., Tahir, M.M., Hassan, M.Z.: Performance investigation of the UTeM Eco-car disc brake. Syst. Int. J. Eng. Technol. **11**(6), 1–6 (2011)
38. Limpert, R.: Brake Design and Safety, 2nd edn, pp. 137–144. Society of Automotive Engineering Inc., Warrendale (1999)
39. Stephens, A.: Aerodynamic Cooling of Automotive Disc Brakes, Masters thesis,.School of Aerospace, Mechanical & Manufacturing Engineering, RMIT University (2006)
40. Zhang, J., Xia, C.: Research of the Transient Temperature Field and Friction Properties on Disc Brakes. In: Proceedings of the 2012 2nd International Conference on Computer and Information Application (ICCIA 2012), pp. 201–204 (2012)
41. Mackin, T.J., Noe, S.C., Ball, K.J., Bedell, B.C., Bim-Merle, D.P., Bingaman, M.C., Bomleny, D.M., Chemlir, G.J., Clayton, D.B., Evans, H.A.: Thermal cracking in disc brakes. Eng. Fail. Anal. **9**, 63–76 (2002)
42. Oder, G., Reibenschuh, M., Lerher, T., Šraml, M., Šamec, B., Potrč, I.: Thermal and stress analysis of brake discs in railway vehicles. Adv. Eng. **3**(1), 1 (2009)
43. Coudeyras, N.: Non-linear analysis of multiple instabilities to the rubbing interfaces:application to the squealing of brake, PhD Thesis, Central school of Lyon-speciality: mechanics (2009)
44. Abu Bakar, A.R., Ouyang, H., Khai, L.C., Abdullah, M.S.: Thermal analysis of a disc brake model considering a real brake pad surface and wear. Int. J. Veh. Struct. Syst. **2**(1), 20–27 (2010)